Feasibility of Pulmonary Airway Tissue Engineering and Repair Using a Cell Spraying Device and Decellularized Porcine Trachea

A THESIS

SUBMITTED TO THE FACULTY OF

UNIVERSITY OF MINNESOTA

BY

Vijay Rajendran

IN PARTIAL FULFILLMENT OF THE REQUIREMENTS

FOR THE DEGREE OF

MASTER OF SCIENCE

Dr. Angela Panoskaltsis-Mortari, Adviser

August 2019

Acknowledgments

I would first like to acknowledge my adviser, Dr. Angela Panoskaltsis-Mortari. I truly appreciated your encouragement and support when I got overwhelmed or thought I couldn't get past a hurdle on this project. Your guidance and advice has taught me a lot about being a better scientist and person that I will take with me into my future endeavors.

To all my colleagues in the Mortari Lab, I appreciated your willingness to help me with different protocols, discuss problems I was having with my experiments, or just provide moments of fun that made working in the lab a good experience. I would like to specifically mention the contributions of Dr. Steven (Steve) Skolasinski, Zachary (Zach) Galliger, and Carolyn Meyer. Steve, thanks for guiding me in what experiments to perform and teaching me different protocols from cell culture to the spraying procedure. Your knowledge and ability to engineer solutions to different problems is admirable. Zach, I appreciated all your help with performing mechanical testing, guiding me through statistical analysis of my data, and assistance with using MATLAB and R/RStudio. Carolyn, thank you for requesting tissue for me almost every week and being able to help with any questions I had.

This project would not have been possible without the help of Dr. Amir Naqwi who developed and built the spraying device. Thanks for always being available to repair the sprayers and discuss any issues. It was an enjoyable experience collaborating with you.

I would also like to thank my other committee members, Dr. Patrick Alford and Dr. Brenda Ogle. It was a pleasure to be in both of your classes. I'm glad I was able to use concepts I learned in both of your courses in my project.

Finally, I would like to thank all my family and friends who supported me in this journey. I wouldn't have made it without you. To my Amma and Appa, thanks for your unconditional support and love. I am grateful for all the hard work and sacrifices you have made so I can have the opportunity to go to graduate school. All the improvements I have made as a person are a credit to you. To my brothers and sister-in-laws, Saravanan Anna, Amanda, Karthi Anna, and Kennie, thanks for your advice and support as I navigated graduate school. And to my nieces and nephew, Mira, Nathan, and Kaavya, you remind me to be joyful for the simple things in life.

Dedication

To my Amma and Appa

For showing me the importance of courage and commitment

ABSTRACT

Methods for tracheal repair and regeneration are necessary due to the limitations of tracheal resection and reconstruction for certain disorders such as tracheal stenosis, tracheomalacia, and tracheal tumors. Additionally, pulmonary injuries such as airway burns do not have effective treatment options aside from supportive care. The feasibility of a cell spraying device is investigated here as a system for applying human bronchial epithelial cells (HBECs) to decellularized porcine trachea matrices for creation of engineered grafts or as a minimally invasive method for delivering cells for wound healing.

HBECs show viability greater than 90% after spraying onto cell culture media or tissue culture plastic. Similarly, one day after spraying onto decellularized trachea, viabilities are seen to be around 90%. Around day three, viabilities were slightly decreased to around 80%. After culturing for over one week, HBECs sprayed onto decellularized trachea displayed a basal cell marker (cytokeratin-5, CK5) and a club cell marker (uteroglobin). Markers for ciliated cells and goblet cells that are crucial for tracheal epithelium could not be found, but this needs to be investigated further. To validate the mechanical performance of the decellularized trachea, compressive resistance testing was performed before and after decellularization of tracheal rings. Results were generally inconclusive with high degrees of variability. A paired sample test conducted with 4 tracheas provided the most interesting results and showed that the decellularization process produced a significantly different compressive resistance compared to the native samples. In practice though this did not seem to be noticeable as the variability found within tracheal samples masked the difference. This would suggest that the decellularization process is not detrimental to the compressive resistance of trachea rings. Based on the results reported here, using a cell spraying device for engineering tracheal grafts and airway epithelial repair seems achievable.

Table of Contents

List of Figures

1. INTRODUCTION/BACKGROUND

1.1 Trachea bioengineering

To understand how to bioengineer a trachea we must first know the necessary anatomy and physiology. The trachea is the main airway that conducts all the air we breathe to and from both lungs[1]. It is vital to the function of the respiratory system and therefore our survival. The trachea has two primary functions: 1) transporting air in and out of the lungs for gas exchange and 2) trapping and removing foreign debris and pathogens found in the airways[2,3].

To properly conduct air, the trachea must remain open under the pressures of respiration[4]. It is a long, rigid tube made up of incomplete cartilage rings connected by a portion of smooth muscle at the posterior of the trachea[1,3,4]. This structure accomplishes two things: 1) stiff cartilage maintains an open airway and 2) smooth muscle allows for flexibility to change shape of the airway. The stiffness of the cartilage rings provides mechanical support by resisting collapse of the airway and maintaining airway patency. Without it, the transmural pressures caused by inspiration and expiration would lead to obstruction of the airway.

The cartilage found in the trachea is known as hyaline cartilage. It is composed of chondrocytes found in lacunae surrounded by dense ECM[2,5]. Chondrocytes secrete the collagens and proteoglycans that make up cartilage and end up trapped in a space called the lacunae[5,6]. Collagen provides the tensile properties seen in the trachea by having aligned fibers circumferentially and longitudinally on the lumenal and ablumenal surfaces[5]. This creates resistance to bending/collapse during periods of forced respiration and allows for longitudinal flexibility which is important for head and neck movement[4,5]. Proteoglycans confer the observed compressive resistance of cartilage because of their large, negatively charged glycosaminoglycan (GAG) side chains and the ability to swell up with water[4,6]. The water contained by the proteoglycans also produces the viscoelastic properties observed in the trachea[7]. Chondrocytes additionally produce enzymes (e.g. matrix metalloproteinases) which are able to break down extracellular matrix (ECM) proteins in order to remodel and renew the cartilage. Compared to other tissues, cartilage is sparsely populated with cells, which limits the need for abundant vasculature.

The smooth muscle connecting the cartilage known as the trachealis changes the shape of the trachea during respiration. This is especially important for physiological events such as coughing which require forced expiration and therefore a sudden change in the shape of the trachea[1,4]. Nerves that connect to the trachealis can also allow for response to altered breathing rates. Additionally, the trachealis is necessary to accommodate the passage of food through the esophagus which lies directly posterior to the trachea.

Although the trachea is primarily composed of cartilage which has a limited blood supply, it has a complicated vasculature because of the epithelial cells found lining the inside of the airway. The main supply comes from arteries which travel longitudinally along both sides of the trachea[1,3,8]. Longitudinal arteries branch off into smaller vessels that travel circumferentially and meet medially around the trachea[1,3,8]. Due to the density of the cartilage, these arteries must travel between the cartilage rings where there is softer fibrous/connective tissue. The intercartilaginous arteries then supply a dense capillary bed found in the submucosal layer of the epithelium to nourish all the cells[1,3,8].

A crucial component of the trachea is the epithelium found in the airway. The tracheal epithelium is composed of multiple cell types and plays a central role trapping and removing foreign debris[2,3,9]. It is composed of three different cell types: 1. basal cells, 2. goblet cells, and 3. ciliated cells[3,9]. The basal cells are epithelial progenitors that have the potential to differentiate into both goblet cells and ciliated cells[9,10]. Research has shown that given proper cues – notably an air-liquid interface culture – basal cells can be differentiated *in vitro*[9]. Goblet cells, named because they resemble a wine goblet, are the cells that secrete mucus to cover the lumen of the trachea[9]. Mucus traps foreign particles and pathogens that can then be expelled from the body through coughing. Ciliated cells form cilia that beat rhythmically to move mucus produced in the lungs and trachea up the airway and out of the body[1,2,9]. This system is called the mucociliary escalator since the mucus is moved unidirectionally through a concerted motion by the cilia[1,2]. Together, the three types of cells form a pseudostratified ciliated columnar epithelium[1,9,10].

As mentioned above, one of the main functions of the trachea is predicated on its mechanical properties. Performing mechanical testing on native tracheal samples can provide information about the characteristics needed for an engineered trachea to perform its biological functions. The mechanical properties of engineered tissues are

vital to the seeding and maturation of cells during recellularization as well. It has been shown by multiple researchers that mechanical cues provided by the scaffold affect differentiation of cells and their behavior in the construct[11–14]. So these data could inform future research on producing mechanically similar scaffolds to native trachea to improve outcomes of engineered trachea.

Clinical need for engineered tracheal constructs comes from multiple disorders, which cause large defects that cannot be repaired with existing tissue. These disorders include tracheal stenosis, tracheomalacia, and tracheal tumors[3,4,15–17]. Tracheal stenosis is a narrowing of the airway that can occur after tracheostomy or intubation in adults and children[16]. Congenital tracheal stenosis is a birth defect found in pediatric patients with the same narrowing. The narrowing can be life threatening as it severely restricts airflow. Tracheomalacia is a disorder where the tracheal cartilage is weakened causing a softer trachea which can lead to closure of the airway during respiration[18]. Tracheal tumors that are removed can also produce a large defect in the trachea[4,15]. Smaller defects (less than 3-4 cm) are typically treated by resection and anastomosing the ends of the remaining trachea[15,19]. Larger defects cannot be treated in this way due to the stress that would be created on the trachea and neck from anastomosing over such a long distance. In adults up to 50% of the trachea can be removed for a procedure while for children only 30% can be removed[3,4]. Additionally, data show that the rate of surgical failure increases as the length of trachea removed increases[19].

Large defects may be treated with organ transplantation. Typically, these are allografts where tissues are transplanted from another human. Allografts are not ideal because of the high risk of rejection after transplantation[2,12,20,21]. To prevent immune rejection these tissues need to be human leukocyte antigen (HLA) matched, but rarely are due to the shortage of donor organs and patients require lifelong immunosuppression[12,14,17]. For pediatric patients, allografts may be unsuitable because the donor trachea has to be the same size as the recipient trachea and donor tissues mainly come from adults. Even if a tracheal graft with the proper size is found, the graft has to be able to integrate with the adjacent tissue and grow with a pediatric patient[2,16,17]. This is why there is a need for engineered grafts that can be made quickly and bypasses using human donor tissue.

A similar approach is using organs from another species to perform a xenotransplant. This method is useful because of the large supply of xenograft tissue

that can be obtained from other animals (particularly pigs)[22]. In the case of pigs, there is also lower risk of disease transmission due to the limited relatedness between pigs and humans[23]. Obviously, this method has serious concerns of rejection because of the foreign biological material present in the organs[22–24]. One way to circumvent this is genetically altering the animal to develop without certain immune-reactive antigens. For example, in pigs the alpha-gal antigen creates an acute immune response in humans. A strain of pig without this antigen has been created by modifying the DNA[22–25]. Another way to reduce the immune response is to use the animals like an “in vivo bioreactor” to produce human organs. This can be done using genetic engineering techniques where a blastocyst of a pig is created without a certain lineage or niche of cells like those that would produce the lung[26]. This missing niche can be replaced by human stem cells or progenitors and as the animal grows the human cells would grow into an adult organ[26]. The organ can then be used for transplant. There are many ethical concerns with this method, so it may not be implemented as a realistic solution.

There are multiple approaches currently being used or studied to create trachea engineered grafts. One approach for developing tracheal grafts is bioprinting. This involves using biomaterials containing cells to 3D print a construct that can be implanted to replace or help regenerate tissue. This method is promising because it allows for careful spatial regulation of cells/growth factors or layering of different types of tissue. Furthermore, the size and shape of the construct can be customized to fit the needs of the patient. Unlike donor grafts, these constructs can be used for children who need an implant that grows with them[2,16,17] or for cases that require a unique implant. The major concern with bioprinting is that the materials being used may not have the mechanical properties necessary to properly carry out tracheal functions. Typically these biomaterials are hydrogels that are not strong enough to maintain the patency of the airway. Synthetic polymers are often used for their superior strength, but they may not provide necessary extracellular cues for cells to properly regenerate the tissue.

Another method is the use of animal or human organs that would otherwise be discarded and engineering them for organ donation. For example, organs from animals that are slaughtered for food would typically go to waste. Some human donor organs are also deemed unsuitable for transplant and go unused. These organs can be decellularized using various methods and then recellularized with human cells to create an organ for transplant. Proper decellularization protocols should remove as much of the

foreign cells and genetic material as possible while maintaining the protein composition and structure of the organ[27,28]. This produces a construct with limited immunoreactivity but conserves important ECM proteins. Retaining the scaffold/ECM of the native organ is advantageous because these proteins are highly conserved across mammals so they can provide important cues for the growth, migration, and maturation of cells[21].

One method of decellularization that has been shown to effectively remove cellular material while preserving ECM proteins is a chemical process using a series of osmotic agents, ionic/nonionic detergents, and enzymes. For decellularizing porcine trachea and lungs, the method involves rinsing with deionized (DI) water, Triton X-100 (Triton), Sodium Deoxycholate (SDC), concentrated sodium chloride (NaCl), deoxyribonuclease (DNase), and then storage in phosphate buffered saline (PBS)[29].

After decellularization, scaffolds can be recellularized using multiple methods. The simplest method is static recellularization, which involves pipetting cells directly onto the scaffold and letting them attach with the help of gravity. For simple tissues with small, flat surfaces this may be suitable. However, many have pointed out that this strategy is ineffective for large, uneven surfaces and hollow/tubular organs[30,31] – many tissues fall under at least one of these categories. Static seeding in these scenarios leads to dripping and pooling of cells which causes an uneven distribution of cells and potentially poor outcomes in tissue engineering applications. The size of the tissue/organ also plays a role into the choice of recellularization method since pipetting billions of cells into a lung, for example, would not be efficient.

Alternatively, dynamic recellularization is the delivery of cells into a scaffold using a pump or bioreactor that continuously perfuses the cells throughout the decellularized scaffold. Theoretically, this allows for full coverage of cells in the construct and further may provide necessary mechanical stimuli for cells as they mature in the construct. For solid organs that contain many different cell types, there is a need for spatially-controlled delivery of cells. In pulmonary tissue engineering, this is where aerosol delivery of cells using a spraying device could be extremely useful similar to delivery of drugs into the lung via aerosol.

Another area of clinical need is the management of inhalational injuries such as airway burns. Around 13,000 to 22,000 people get inhalational burns each year in the United States[32]. This leads to increased morbidity and mortality for patients and leads to worse outcomes when not treated properly[33,34]. A key component of inhalational injury is

loss of the airway epithelium which leads to inflammation and potential infection, airway obstruction, and stenosis[33,34] . With supportive care, it takes about 3 weeks for the native epithelium to fully repair the damaged area[33]. By having a minimally invasive method to deliver epithelial cells to airway burn patients, the airway lining could be healed quickly and outcomes could be improved. Again, spray delivery of cells may be a solution.

Although these disorders and subsequent procedures are relatively rare, developing improved methods for treatment would immensely help those patients who need it. The research performed in this thesis investigates the feasibility of using a spray device in trachea tissue engineering as a proof of concept for airway engineering and other pulmonary applications.

1.2 Cell spraying

An alternative method of seeding which has become increasingly studied is using a cell spraying device to deliver cells. Several researchers have used this approach for different applications including epidermal and burn wound healing[31,35], intestinal epithelialization[30], bladder regeneration using demucosalized colon[36], and delivery of airway epithelial cells or MSCs for treatment of airway/lung injury[37–39]. The latter method is further studied here as a potential avenue for recellularization in pulmonary tissue engineering. Although airway epithelial cells and MSCs have been sprayed *in vitro* onto tissue culture plastic or biomaterial surfaces (gelatin) or *in vivo* into a rabbit model of airway injury, it has yet to be shown that airway epithelial cells can be sprayed onto decellularized trachea scaffolds as a method for airway engineering. By demonstrating this, use of cell spraying could be translated to recellularizing whole, decellularized porcine lungs.

The sprayer is made with two flexible, plastic tubes that create an outer lumen and inner lumen. Compressed air is introduced through the inner tube and the liquid cell suspension is instilled through the outer lumen. Near the sprayer end, there is a short metal tube which is attached to the inner tubing and contains holes in the side. Liquid enters the inner lumen through these holes and is perturbed by the air. The disturbance in the liquid phase leads to a breakup of the flow into ligaments which further break up into droplets[40]. This interaction between the liquid and air creates an aerosolized spray outside the device.

The major benefit of using a cell sprayer is the ability to distribute cells across a large, contoured surface and inside of hollow, tubular organs[30,31,35,37]. Because of the cone-like shape of the spray pattern, this device should provide better coverage when reepithelializing airways compared to a static recellularization method. When combined with adhesive biomaterials, such as fibrin, pooling and dripping encountered with static seeding on unfavorable topographies can be overcome[30,31,35,41].

Another benefit for pulmonary applications is delivery of cells into proximal and distal areas of the lungs. The size of the device makes it possible to be used in smaller airways since it can be advanced down multiple generations of the bronchial tree. This is useful since a major issue with current recellularization approaches is the delivery of cells to distal parts of the airway to recapitulate the alveolar-capillary unit[42]. These areas are often difficult to access due to the narrowing of the bronchioles, which can easily lead to blockages. Others have also shown that this type of spraying device can be incorporated into an endoscopic device[30,37,40]. This would allow for targeted, on-demand application of cells during diagnostic and surgical procedures[30].

Spraying also affords spatial variability in cell distribution and layering of different cell types. This is important in pulmonary airway engineering since different areas of the lung have different compositions of cells in the epithelium. Using a sprayer, these cellular compositions could be matched along the airway tree. Spraying multiple layers of cells could recreate a pseudostratified epithelium that is characteristic of the airways.

Aerosol deposition of cells is compatible with an air-liquid interface culture. This condition is important especially for the generation of functional airway grafts. Air-liquid interface is often used for differentiation of airway epithelial cells. Thiebes et al. have shown that respiratory epithelial cells can be sprayed onto transwell inserts and cultured in an air-liquid interface for 28 days producing goblet cells and ciliated cells[37].

There are potential applications for delivering soluble drugs (like pulmonary surfactant), cellular therapies, or growth factors to improve tissue engineering. The delivery of pulmonary surfactant has been studied as an application for newborns with respiratory distress syndrome[43]. Aerosol delivery is attractive in this scenario since the spraying device is small enough to be used in premature patients while also delivering the surfactant at a low pressure and low flow rate to limit trauma to the newborn. Cellular therapies for pulmonary alveolar proteinosis (PAP) or lung regeneration may also benefit from spray delivery of cells. PAP is caused by a defect present in macrophages of the

alveoli. Genetic correction of patient-derived macrophages[44] or iPSC-derived macrophages[45,46] can return the cells to a normal functional state. Spray delivery of these cells would allow for homogeneous distribution into the alveoli as a therapeutic for a diseased patient. Lung regeneration after injury has also been studied using sprayed MSCs as a cellular therapy[39].

Finally, the device could be used to seed cells onto completely different tissues like delivering endothelial cells to the lumenal surface of vascular grafts, or epithelial cells to the surface of the gastrointestinal tract.

2. EXPERIMENTAL METHODS/MATERIALS

2.1 Cell culture

Human bronchial epithelial cells (HBECs) were obtained from Promocell (Heidelberg, Germany). Cells were cultured using Airway Epithelial Cell Growth Medium (Promocell). This was made by mixing Airway Epithelial Cell Growth Medium SupplementMix (C-39165, Promocell) with Airway Epithelial Cell Basal Medium (C-21260, Promocell). The media was supplemented with 1 mL of Primocin (ant-pm-2, InvivoGen, San Diego, CA) as an antimicrobial agent. Cells were incubated at 37°C and 5% CO_2 with media being changed every 2-3 days. Cells were harvested for spraying by removing media, rinsing with PBS, and incubating with TrypLE Select (Thermo Fisher Scientific, Waltham, MA) to dissociate from culture flasks. Cell suspensions were centrifuged at 1200 rpm for 5 minutes. Subsequently, supernatants were aspirated being careful not to disturb the cell pellet. Cells were resuspended in growth media at a concentration of 1-5 million cells/mL prior to seeding and spraying experiments.

A549s were obtained as a generous gift from the Daniel Vallera lab (University of Minnesota) and cultured with D10 media. Skin-derived fibroblasts were obtained as a generous gift from the Jakub Tolar lab (University of Minnesota) and grown with fibroblast media. RFP-positive HUVECs were obtained from Angio-Proteomie (Boston, MA) and grown using endothelial cell media from R&D Systems (Minneapolis, MN).

2.2 Obtaining porcine trachea

Porcine tracheas were obtained from the Visible Heart Lab (VHL, University of Minnesota, Minneapolis, MN), Advanced Preclinical Imaging Center (APIC, University of Minnesota), or Hormel Foods (Austin, MN). Connective tissue was removed from the

ablumenal side of the trachea. Tracheas were then either stored as native samples for use in mechanical testing or decellularized for use in spraying experiments and mechanical testing. Native trachea samples were stored in PBS at 4°C until use.

2.3 Decellularization of porcine tracheas

After removal of connective tissue, intact tracheas for decellularization were sequentially incubated with a series of reagents on a shaker plate. The trachea was incubated with approximately 500 mL of DI water overnight at 4°C. DI water was drained and the trachea was incubated with approximately 500 mL of 0.1% Triton X-100 (Sigma-Aldrich, St. Louis, MO) for 24 hours at 4°C. Triton was drained and the trachea was incubated with approximately 500 mL of 2% SDC (D6750, Sigma-Aldrich) for 24-48 hours at 4°C. Length of incubation for the SDC step was determined based on visual inspection of the trachea to assess degree of decellularization. SDC was drained and the trachea was rinsed with approximately 500 mL of concentrated (1 M) NaCl (S9625, Sigma-Aldrich) for 24 hours at 4°C. NaCl was drained and the trachea was rinsed with approximately 500 mL of 30 µg/mL bovine pancreatic DNase (10104159001, Roche Diagnostics, Indianapolis, IN) in 1.3 mM $MgSO_4$ and 2 mM $CaCl_2$ overnight at 4°C. Finally, the DNase solution was drained and samples were stored in 500 mL PBS at 4°C. After discovering that contamination of the decellularized tissues was leading to cell death in seeding experiments, samples were stored in 500 mL PBS with 1x penicillin-streptomycin (pen-strep) (15070-063, Thermo Fisher Scientific). This is discussed further in section 3.3.

2.4 Seeding cells onto decellularized porcine trachea

Decellularized porcine tracheas were cut into 1-2 cm wide rings. Rings were then cut open through the trachealis and 1-2 cm pieces were cut from cartilage rings. Trachea pieces were placed into wells of a 24-well plate and soaked in Airway Epithelial Cell Growth Medium overnight at 37°C. Before seeding, soaked trachea pieces were moved to empty wells of a new 24-well plate. Cell seeding was then performed by pipetting cell suspension directly onto the decellularized scaffold pieces.

In certain experiments, fetal bovine serum (FBS, HyClone/GE Healthcare, Chicago, IL) and human platelet lysate (PLTMax, Mill Creek Life Sciences, Rochester,

MN) were used as 2% supplements to the cell culture medium or for incubating with the decellularized tissue overnight.

In other experiments, collagen and fibronectin were used as coatings for the decellularized trachea scaffolds. Collagen, Type I solution from rat tail (C3867, Sigma-Aldrich) was diluted with water for injection (WFI) to 0.01% (v/v). Human fibronectin (354008, Corning, Corning, NY) was diluted to 50 µg/mL with cell culture media. Tissues were incubated with approximately 250 µL of collagen or fibronectin at room temperature for 4 hours. Excess solution was aspirated and the tissue was rinsed with cell culture media prior to seeding.

2.5 Spraying

2.5.1 Sprayer setup

A catheter-based spraying device (Abbe Vision, Minneapolis, MN) was connected to a syringe pump (Pump 11 Elite, Harvard Apparatus, Holliston, MA) and a generic airbrush compressor. The syringe pump was used for instilling the cell suspension into the outer lumen of the sprayer. The airbrush compressor was used to deliver air to the inner lumen of the sprayer. A HEPA filter was connected to the airbrush compressor to filter the air prior to its connection to the sprayer. Figure 2.1 shows images of the setup.

2.5.2 Trachea pieces in 24-well plate

Decellularized porcine tracheas were prepared as described in section 2.3 and 2.4. Prior to spraying, 70% ethanol was run through the sprayer to clean it. Next, DI water was run through the sprayer to remove any residual ethanol. After the sprayer became clogged multiple times, it was determined that using ethanol to clean the sprayers was degrading the epoxy and creating blockages. From then on, only warm DI water was used to clean the sprayers. After cleaning, the sprayer was primed with cell suspension and preliminary sprays were performed without a substrate to obtain consistent sprays. Trachea pieces were then sprayed at a pressure of 30 psi using a volume of 100-250 µL to obtain a seeding density of 100,000-400,000 cells/cm^2. To spray tracheal pieces, the air valve was first opened and the syringe pump was started as quickly as possible. After the spray volume was injected, the air valve was left open for approximately 5 seconds to spray residual volume of cell suspension. Then, the air

valve was closed, the sprayer was moved to the next sample, and the process repeated until all samples were sprayed. Cells sprayed into empty wells and cells dispensed through the sprayer (without air flow) were used as controls.

2.5.3 Intact trachea segment in upright bioreactor

To determine the feasibility of spraying in a clinically relevant setting, spraying was performed into upright trachea segments inside of a custom mini-bioreactor (Figure 2.2). Mini-bioreactors were created using 35mm x 10mm tissue culture dishes (229635, CELLTREAT, Pepperell, MA) and 50 mL conical tubes (352070, Corning). Conical tubes were cut down to approximately 3 cm long using a handheld rotary tool kit. These pieces were attached to the bottom of the petri dish using Loctite Super Glue Gel Control (Henkel, Rocky Hill, CT). Super glue was allowed to dry overnight. Mini-bioreactors were gas sterilized prior to use. Decellularized porcine tracheas were cut into 2 cm long segments. Trachea segments were blotted using kimwipes to remove all excess moisture. Segments were attached to the bottom of the mini-bioreactors using 2% low melt agarose (E-3126-125, BioExpress, Kaysville, UT). Agarose was allowed to set for 1 hour at room temperature to ensure attachment.

Spraying was then performed in similar manner as described above. Lower volumes (50-100 µL) were used to limit pooling and dripping of the cell suspension in the bioreactor. Cell concentrations were increased to maintain the same seeding density as described above. In the final experiment, fibronectin was sprayed to coat the inside of the tracheal rings using the same concentration as described in section 2.4.

2.6 Culture and imaging

After spraying of cells, trachea pieces were moved into wells with 0.75-1 mL of growth media. This was done – rather than adding media directly on top of the sprayed pieces – to minimize washing away cells from the surface of the trachea. Media was changed 24 hours after spraying and subsequently every other day. Samples were imaged at multiple time points using the LIVE/DEAD viability/cytotoxicity kit (Thermo Fisher Scientific, Waltham, MA). Briefly, the LIVE/DEAD stain was prepared following the manufacturer product sheet to make a 2 µM calcein AM and 4 µM ethidium homodimer-1 (EthD-1) solution in PBS. Media was aspirated from the wells and samples were incubated in 250-300 µL of LIVE/DEAD stain (enough to cover the top of the

tissue) for 15 minutes at 37°C. After staining, tracheal samples were moved to wells containing 250 µL of PBS with the sprayed surface facing the bottom of the plate. Samples were imaged using the EVOS FL Auto 2 (Thermo Fisher Scientific) fluorescent microscope with GFP and RFP light cubes. Images were captured at 4x, 10x, or 20x across different areas of samples.

2.7 Quantification of cell viability

Cells were counted using a custom-made semi-automated ImageJ plugin. Briefly, raw images from each fluorescent channel (GFP and RFP) were counted separately using the plugin which ran a series of functions including background subtract. Particles were counted with minimum and maximum particle sizes based on the magnification of the image. Outlines of the particles counted were merged with the subtracted background image to visually verify that the plugin was appropriately counting cells. Additionally, manual counts were performed when feasible to validate the cell counts.

2.8 Histology

2.8.1 Freezing blocks

At different time points, samples were frozen for histology and staining. Samples were placed upright (so that sections would be transverse) in small aluminum foil cups containing Tissue-Tek O.C.T. (optimal cutting temperature) compound (Sakura Finetek USA, Torrance, CA) and frozen using liquid nitrogen. Frozen tissue blocks were stored at -80°C until ready for sectioning.

2.8.2 Sectioning

Tissue blocks were placed in the Leica CM1900 cryostat (Leica Biosystems, Buffalo Grove, IL) 30 minutes prior to sectioning to allow the blocks to equilibrate to the proper cutting temperature. Porcine trachea blocks were sectioned at -13 to -16°C. Mouse lung blocks – used as positive controls for uteroglobin and surfactant protein C staining – were sectioned at -10 to -13°C. 10 µm sections were cut from blocks and 2 sections were adhered to each slide. 10 sections were taken as a group in serial succession. After a group of sections, the cryostat was advanced approximately 1 mm further into the block and the next group of sections was taken. In total, approximately 40-50 sections were taken from each block. One slide from each group of slides was

taken for H&E staining. The rest of the slides were either stored at -80°C or immediately used for immunofluorescent staining.

2.9 Immunofluorescent staining

Slides were removed from -80°C and allowed to come to room temperature for about 20 minutes. Optimal protocols were determined by using information from the product datasheet, paper references, and experimental trials. The protocols for each antibody are described below. Staining was carried out in a dark, humid chamber created by using a plastic box with wet paper towels on the bottom. Slides were elevated on a rack in the box.

2.9.1 Cytokeratin 5 (CK5)

Sections were fixed by covering them with 4% paraformaldehyde for 10 minutes at room temperature. Slides were rinsed with PBS. Sections were then permeabilized with 0.1% Triton X-100 for 5 minutes. Slides were rinsed with PBS. Sections were blocked with Normal Serum Block (Biolegend, San Diego, CA) for 1 hour at room temperature. Slides were rinsed with PBS. Sections were then incubated with rabbit monoclonal antibody to human CK5 conjugated with Alexa Fluor 488 (1:250 dilution, ab193894, Abcam, Cambridge, UK) at 4°C overnight. Control slides were incubated with PBS to prevent dehydration of sections (no primary antibody). Slides were rinsed with PBS. Coverslips were mounted using VECTASHIELD Hardset Antifade Mounting Medium with DAPI (H-1500, Vector Laboratories, Burlingame, CA) to counterstain cell nuclei. Slides were left out to dry for 15 minutes and then imaged using the EVOS FL Auto 2.

2.9.2 Uteroglobin

Sections were fixed by covering them with 4% paraformaldehyde for 10 minutes at room temperature. Slides were rinsed with PBS. Antigen retrieval was then performed by placing slides in citrate buffer (pH 6) heated to 90°C using a water bath for 10-20 minutes. Slides were rinsed with PBS. Sections were blocked with Normal Serum Block (Biolegend, San Diego, CA) for 1 hour at room temperature. Slides were rinsed with PBS. Sections were then incubated with rabbit polyclonal antibody to human uteroglobin cross-reactive with mouse and rat (1:250 dilution, ab40873, Abcam, Cambridge, UK) at

4°C overnight. Control slides were incubated with PBS to prevent dehydration of sections (no primary antibody). After overnight incubation, slides were rinsed with PBS. All slides were then incubated with Cy3 AffiniPure Donkey Anti-Rabbit IgG secondary antibody (1:750 dilution, 711-165-152, Jackson ImmunoResearch Laboratories, West Grove, PA) for 1 hour at room temperature in the dark. Slides were rinsed with PBS. Coverslips were mounted using VECTASHIELD Hardset Antifade Mounting Medium with DAPI (H-1500, Vector Laboratories) to counterstain cell nuclei. Slides were left out to dry for 15 minutes and then imaged using the EVOS FL Auto 2.

2.10 Mechanical testing

Decellularized porcine trachea or native porcine trachea was cut into approximately 1 cm wide rings, unless otherwise stated (one experiment had 2 cm wide rings). Depending on the size of the trachea, anywhere from 5 to 13 samples were obtained from each trachea. The portion of the trachea with the first branching above the carina – found in pigs but not humans – was excluded from mechanical testing to maintain uniformity between samples. Mechanical testing was performed on a Mach-1 tester (V500CSST, Biomomentum, Laval, Quebec, Canada). Samples were attached to the testing platform using Loctite 4013 Instant Adhesive (Henkel, Rocky Hill, CT) with the smooth muscle (trachealis) of the trachea on the surface of the platform. Tracheal rings were compressed using either a 12.5 mm diameter flat indenter (MA262, Biomomentum) or a 31.75 mm diameter flat indenter (MA263, Biomomentum).

Before compression, a “Find contact” function was performed using the mechanical tester to find the surface of the tracheal ring with the indenter. This gave a height for the ring which was used to measure the force at 50% displacement of the samples. That measure was used to compare the compressive resistance between samples. Rings were compressed at a rate of 0.2 mm/s (roughly 1% of the sample height per second)[47]. Samples were compressed to 75% of the height determined using the “Find contact” function. Generally, this meant samples were fully occluded at the end of testing. Images of compressive mechanical testing are shown in Figure 2.3.

2.11 Statistical analysis

A one-way ANOVA using R/RStudio was performed on data sets with more than two groups for comparison. If the ANOVA determined there was a significant difference

between two different groups, post-hoc analysis was performed using a Tukey HSD test for all pairwise comparisons. When only two different groups were compared, a two-tailed t-test using Excel was performed. P-values less than 0.05 were deemed to be significant.

3. RESULTS

3.1 Compressive resistance mechanical testing of native vs. decellularized porcine trachea

After decellularization of porcine tracheas, the compressive resistance was compared to native tracheas using a mechanical tester to observe how the decellularization process would affect the mechanical properties. By measuring the compressive properties, the resistance to collapse of the trachea can be compared. Since tracheal collapse is a major concern after surgery, it is important to know that the decellularized scaffold can be as strong as the native trachea.

The first mechanical test was performed as a sequence of stress relaxations (results not shown). Stiffness of the trachea was calculated and plotted as a function of the percent compression. Up to 30% compression, the stiffness of the native and decellularized tracheal rings was identical. From 40% to 70% compression, the native samples were slightly stiffer, but due to the variation in samples there appeared to be no difference between both groups. It was thought this setup would provide information about the aggregate modulus of the tracheal cartilage. However, due to the samples being rings, it was difficult to measure the area over which the load was being distributed to calculate an accurate stress.

Following previous literature[47,48], the compressive testing method was changed to the description in section 2.10. The next experiment was performed using the new method and resulted in a higher average compressive resistance for native samples than decellularized samples (Figure 3.1). A large standard deviation in the decellularized group meant that the result was not statistically significant after performing a two tailed t-test assuming unequal variances ($p=0.24$). However there are only 3 samples in each group and all the samples were taken from one trachea so it is difficult to conclude anything. Samples were also around 2 cm in width which is larger than the small plate indenter used for testing. This could lead to edge effects that are not indicative of the trachea properties.

To limit edge effects, tracheal rings were cut to 1 cm in width for the next experiment. Samples were also ordered from proximal to distal and tested to note whether there are any differences in compressive resistance along the length of the trachea. There seems to be a trend of increasing compressive strength from proximal to distal for the native tracheal samples, but a decreasing compressive strength for the decellularized tracheal samples (Figure 3.2). The average force for the native group is also significantly higher than the decellularized group after testing with a two tailed t-test assuming unequal variances ($p=4.7x10^{-6}$, Figure 3.3). An important caveat is that these samples were not kept hydrated in PBS during the sample processing and immediately prior to testing which may affect the results.

To control for variability from edge effects with a small indenter, a large indenter was used in future experiments. The next experiment was performed with trachea obtained from APIC and samples were kept hydrated in PBS immediately prior to testing. Generally, the native trachea showed a higher compressive resistance compared to the decellularized trachea across the length of the trachea (Figure 3.4). However, there is a lot of variability present in both groups. Particularly, the first sample of the decellularized trachea was over 0.5 N stronger than the strongest native trachea sample. This meant after averaging across all samples and performing a two tailed t-test assuming unequal variances the data was not statistically significant ($p=0.166$, Figure 3.5). Also, both groups show a decreasing trend from proximal to distal along the trachea which was not seen in the previous experiment. Sample hydration may explain these discrepancies. These differences may have to do with the different source of trachea and larger indenter as well.

Experiments with tracheas from Hormel Foods using the large indenter show similar results. All tracheas display a slight decreasing trend in compressive resistance as expected since the trachea is much stiffer near the larynx (Figure 3.6). After pooling the native and decellularized trachea and performing a two tailed t-test assuming unequal variances the data was not statistically significant ($p=0.199$). Because the animals from Hormel Foods were larger than other sources, the compressive resistance of the tracheas was also higher. Therefore, it is not reasonable to compare the absolute forces across tracheas due to the different sizes of animals. Gender and strain of pig may also affect the compressive resistance of the trachea.

To control for these variables and more accurately measure the effect of the decellularization process, samples were paired in future experiments. With this new experimental design, decellularized samples generally followed the same trend as the native paired samples but at a lower strength. This can be seen in Figure 3.8 where the values are averaged and grouped by trachea. By calculating the mean difference in compressive resistance it seems that native trachea samples are significantly different from decellularized tracheal samples. Analyzing the data with a paired two sample t-test confirms this. All tracheas are statistically significant (trachea 1, $p=0.043$; trachea 2, $p=0.0027$; trachea 3, $p=0.0037$; trachea 4, $p=0.00067$). This suggests that the decellularization process does have an effect on the mechanical properties of the trachea.

3.2 HBECs maintain high viability after spraying onto multiple types of substrates

To show that HBECs could be applied to decellularized tracheal pieces via spraying, it first had to be shown that human bronchial epithelial cells could survive the spraying process. This was done by spraying cells into a well plate with or without culture media. Spraying into a well with culture media is a relatively soft surface for the cells to land on while spraying onto the empty well plate is a rigid surface for the cells to land on. Based on work previously done in the lab to characterize the sprayer, it was found that there were general values for the air pressure and liquid flow rates to obtain a proper spray. The range for the air pressure was between 10 and 30 psi and the liquid flow rate was around 0.2 mL/min. This produced droplet sizes with a mean diameter of 30 μm and average velocities ranging from 8.5-13.5 m/s. Previous spraying experiments with these parameters showed greater than 90% viability. Subsequent experiments performed with newer sprayers at 1-2 mL/min and 30 psi were consistent with previous results. After 1 day, cells show good attachment after spraying into media at 2 mL/min (Figure 3.10) and there is no significant change in viability between the sprayed groups and the non-sprayed group (sprayer 1 to no-spray: $p=0.743$, sprayer 2 to no-spray: $p=0.382$). However, there was a significant difference in viability between the two sprayers tested (sprayer 2 to sprayer 1: $p=0.0295$). Although there is a statistical difference between the two sprayers, there is still a high viability, around 90%, for sprayer 2 (Figure 3.11). This suggests that the practical effect may not be significant. The variability seen between sprayers is likely due to the sprayers being custom-made.

What this confirms is the need for an automated, quality control process for building clinically applicable sprayers. Images in Figure 3.10 are representative of results obtained from two experiments testing two different sprayers.

To reinforce the conclusion that HBECs have a high viability after spraying, another experiment was performed where viability was determined 1 hr after spraying rather than 1 day later to eliminate the potential confounding effects of cell proliferation. Since these data were gathered at 1 hour vs. 1 day, it may be more indicative of the direct effects of the sprayer on the cells. Data taken after 1 day may capture the proliferation of cells rather than the direct viability of cells after spraying. HBECs were sprayed at 1 mL/min onto decellularized trachea pieces, into wells with media, and into empty wells. All conditions show greater than 95% viability and there is no significant difference between the three groups ($p=0.837$, Figure 3.12).

These data show that cells can survive the stresses of flowing through the sprayer, being aerosolized, and landing on different types of substrates. These preliminary experiments also show that cells can be cultured after spraying without contamination and sprayers can be used multiple times.

3.3 Seeding of HBECs onto decellularized trachea pieces

Prior to spraying, cells were seeded onto decellularized trachea pieces via pipetting to ensure that cells could be grown on the tissue. The first experiment was performed with HBECs only on decellularized trachea pieces and shows the importance of seeding density. After LIVE/DEAD staining, no cells can be found on any of the tissue samples (Figure 3.13b), but with such a high seeding density many cells are dead even in the cells-only control (2.4 million cells/well). Subsequent experiments were performed with additional cell types to observe differences in seeding and identify whether the cause of cell death was related to the cell type.

In the next experiment, the seeding density was decreased to approximately 500,000 cells/well. Again no living cells were seen on the tissue samples (Figure 3.13c). Fibroblasts were also added to the experimental conditions and showed similar results (images not shown). The control condition was similar across multiple seeding densities and cell types. The experiment was repeated with a seeding density of 100,000 cells/well (Figure 3.13d) and showed similar results.

A549s were added to the experiments to see if there would be a difference in the seeding. A new trachea was also used for the seeding procedure. For this experiment images were taken at shorter timepoints (3 hrs and 24 hrs) to see when the cells were dying. Because tissues incubated with LIVE/DEAD stain cannot be cultured further, images at the 3 hr timepoint and 24 hr timepoint are from different tissue pieces. Again, cells look healthy in the cells-only control wells. At 3 hrs there are cells on the tissue in the A549 and HBEC conditions, however there are also many dead cells (Figure 3.14). At 24 hrs there are HBECs on the tissue but they still do not appear to be healthy compared to Figure 3.17. There are no viable fibroblasts on the tissues at either time point.

To observe whether seeded cells were dying in the incubation well due to something in the tissue, or not attaching to the tissue and attaching to the bottom of the incubation well, live/dead images were taken of the incubation wells after removal of the tissue. Wells were also imaged after staining to see if many cells were being removed from the tissue during the staining process. Very few cells were seen (data not shown) and most were dead, consistent with the results on the tissue, but did indicate that cells were not coming off the tissue.

To further explore whether cells being in contact with the tissue was leading to cell death, an experiment was performed where HBECs were either seeded onto decellularized trachea pieces or cocultured in a well with decellularized trachea without being directly on the tissue (Figure 3.15). At 1 hr there are many cells alive in both tissue and coculture conditions. Based on the rounded morphology of the cells, they still have not attached to the tissue or culture plate. At 2 hrs there are very few cells found on the tissue and those that are there are not viable. However, the coculture condition shows that cells are alive in the well and even surviving right next to the tissue. The morphology of the cells has also changed as the cells have had enough time to attach to the tissue or plate. Finally, at 18 hrs there are almost no viable cells on the tissue. Unlike earlier time points, the coculture condition also shows many dead or dying cells. These cells have also returned to a rounded morphology as they have detached from the plate.

In an attempt to improve survival and attachment of cells to tissue, fetal bovine serum (FBS) and platelet lysate (PLTMax) were tested as supplements to media during the seeding process. Multiple experiments were performed with FBS/PLTMax using differing conditions. HBECs were seeded onto decellularized trachea with FBS and

PLTMax supplementing the culture media. Subsequently, HBECs were also seeded onto decellularized porcine lung pieces. In a final experiment, decellularized trachea pieces or decellularized porcine lung pieces were soaked in FBS or PLTMax prior to seeding with cells. These samples were then cultured with cell culture media after seeding. Other experiments with the addition of collagen or fibronectin to the surface of the decellularized tissue were also performed in an attempt to improve the attachment of cells.

Addition of FBS or PLTMax as a supplement to the media did not improve seeding outcomes as there were very few viable cells (Figure 3.16). Soaking the tissues in FBS or PLTMax prior to cell seeding did not significantly improve results. Interestingly, cells cultured in the decellularized trachea-conditioned medium also did not survive indicating that something from the tissue was altering the media to make it inhospitable to the cells (Figure 3.16). The addition of collagen or fibronectin to the tissues did not make any difference as there were few, if any, viable cells (images not shown).

After observing that cells were dying after seeding into wells without tissue but only the conditioned medium from decellularized trachea, it was hypothesized that something was being leached from the tissue. One idea was that residual detergent left from the decellularization process was not being thoroughly washed away and was being released into the media during soaking which led to cytotoxicity. To determine the detergent content of the tissues, a residual detergent assay was attempted as previously described[49], but a cytotoxic presence of detergent could not be demonstrated.

Throughout the previous experiments, it was observed that the color of the cell culture media would change rapidly (from pink to orange/yellow) indicating a drop in pH typically due to high metabolic activity of cells or bacterial contamination – but no contamination was evident. The pH was found to be around 6, which is below normal physiological pH of 7.2 – 7.4. To correct this, an assay with HEPES was performed to buffer the media from pH change. Different concentrations of HEPES were added to the media from 15 mM, 25 mM, 35 mM, and 45 mM to see if pH could be maintained and the cells would survive. Addition of HEPES at any concentration did not change outcomes of seeding and there were no viable cells on the tissues (images not shown).

After many attempts using different cells and other types of decellularized tissues, samples were left to incubate longer and contamination did indeed appear. It was concluded that contamination of tissue may be the reason for cell death during the

experiments. Storing decellularized tissue in antibiotics (pen-strep) prior to cell seeding resulted in adherence of viable cells that could grow to confluency on the tracheal tissue (Figure 3.17).

3.4 Successful application of HBECs onto decellularized tracheal pieces using sprayer device

After solving the issue of cells dying and optimizing the seeding protocol, human bronchial epithelial cells were sprayed onto decellularized trachea pieces (Spray – trachea). HBECs sprayed into media (Spray – media), pipetted onto trachea (Pipette – trachea), and pipetted into media (Pipette – media) were used as controls. Multiple experiments were performed with representative LIVE/DEAD staining images shown in Figures 3.18 and 3.19. Coverage of cells in the first experiment (images not shown) appeared to be sparse at the early time points (24 hrs and 48 hrs). This improved with time, however, as there was better coverage at day 3 which may be due to proliferation of cells. Viability in the first experiment is above 80% for 24 hrs and 72 hrs but around 75% for 48 hrs (Figure 3.20). The high variability for the day 2 sample indicates that there are certain areas of the tissue with low cell viability and other areas with high cell viability. These viabilities are lower than the cells-only control and the pipette-seeded trachea control at 72 hrs Statistical analysis was performed after grouping samples by day. The only test that was statistically significant was on day 3 between the sprayed trachea and the pipette-seeded trachea ($p=0.0144$, Figure 3.20).

The second experiment shows much better coverage of cells at 24 hrs and 72 hrs (Figure 3.18). Also, viabilities at these time points are above 80% (Figure 3.21). The sprayed trachea sample at day 1 is statistically different from the spray media sample ($p=0.0152$). At day 8, the viability drops to around 40% which is significantly lower than all other groups at the same time point (Spray trachea-Spray control media, $p=0.0014$; Spray trachea-Pipette control trachea, $p=7.81\times10^{-5}$; Spray trachea-Pipette control media, $p=3.52\times10^{-4}$). It is possible this is due to some variability caused by the spraying procedure or culturing of tissues and not necessarily because of the sprayer itself. For example, tissue pieces sprayed near the end of the spraying process may not receive the same number of cells as those at the beginning or middle. Throughout the spraying, cells may settle inside the syringe leading to a lower concentration that is sprayed. In this experiment, the sprayer began to produce an abnormal, erratic spray pattern with some of the spray landing outside of the intended wells. This could easily explain why

the sprayed tissues at day 8 have many fewer cells compared to the tissues with pipetted cells.

In the final experiment (Figure 3.19), there is moderate coverage at the early timepoint (72 hrs) compared to the later timepoint (day 6). Although in both cases, the viability is above 80% (Figure 3.22). At day 6 there is very good coverage of the tissue, most likely due to proliferation of cells, with small areas throughout the tissue still lacking cells.

3.5 Sprayed HBECs on trachea pieces express lung epithelial cell markers

Three spray experiments were performed with tissue pieces cultured up to 9 days. Samples from these experiments were frozen and sectioned. Some samples were stained with hematoxylin and eosin (H&E) to observe cells on the surface of the sprayed tissues. Representative images of H&E staining are shown in Figure 3.23. Cells show good coverage across the tissue as there is a continuous layer of cells (solid arrows) on the epithelial membrane. Some samples also show what appears to be pseudostratification as some cells are in different layers. When compared to a native human trachea (images not shown), epithelial cells in the native trachea have a much more polarized architecture with cells appearing elongated, containing cilia, and facing directly outward from the epithelial surface (apical-basal polarity). However, cells in the sprayed sample are simply layered on top of one another and do not show signs of cilia.

Other samples were immunofluorescently stained for pulmonary epithelial cell markers CK5 and uteroglobin. HBECs express the basal cell marker, CK5, even 8 days after being sprayed onto decellularized trachea pieces (Figure 3.24). The staining appears almost identical to the positive control samples (native porcine trachea). HBECs also express the club cell marker, uteroglobin, 8 days after being sprayed onto decellularized trachea pieces (Figure 3.25). Sprayed samples show some diffuse staining in the cartilage closer to the epithelial layer. This staining is not seen in the negative control (sprayed samples with secondary antibody only). Positive control samples (adult mouse lung) show a similar diffuse staining as seen by the hazy fluorescent signal surrounding the bronchioles where uteroglobin is expected. This type of staining is likely due to uteroglobin being a secreted protein.

3.6 Spraying onto intact trachea using a vertical mini-bioreactor

After having success spraying onto decellularized trachea pieces in a well plate, spraying was attempted on complete tracheal segments in an upright position. The goal of this was to show that spraying could be carried out in a clinically relevant setting where the trachea is intact and the orientation of the tissue may not be conducive to cell adhesion. In all previous spraying experiments, tracheal tissue pieces were in a well plate with the sprayed surface facing up. This meant that gravity aided in the seeding process. Clinical applications would not necessarily allow for this as there may be different orientations and topographies to spray onto.

Unfortunately there was not any success in delivering cells onto the scaffold this way. Because of gravity, the cell suspension that was sprayed onto the tissue would pool at the bottom of the mini-bioreactor. Even after spraying lower volumes (50-100 µL) with higher cell concentrations, outcomes were similar and there were no cells attached to the scaffold. This could be due to the high cell concentrations, which may have led to clumping of cells, or the liquid volume is still too high. An experiment to improve cell adhesion was performed by spraying fibronectin onto the surface of the scaffold prior to spraying HBECs. This did not lead to improved outcomes for cell attachment.

4. DISCUSSION

4.1 Compressive mechanical testing of decellularized porcine trachea is inconclusive

As mentioned in Section 1.1, the mechanical properties of the trachea are important because of its function in maintaining a patent airway. Therefore, measuring the compressive resistance of decellularized porcine trachea is necessary when creating engineered tracheal grafts. It is important to keep in mind that these results are based on *in vitro* testing of tracheal rings. Removal of the trachea from the native state will significantly alter the mechanics since connective tissue supports and anchors the trachea. However, this can provide some information on the effects of the decellularization process on the scaffold and important factors for future studies on trachea mechanics.

After reading previous literature on mechanical testing of trachea[47,48], it was decided that the method of multiple stress relaxation steps was not the best way to

measure the physiologically relevant mechanical properties of the trachea. Although this method can provide data about the viscoelasticity of the trachea, it does not accurately describe the compressive resistance of the trachea since the sample is allowed to relax at each step of the compression. Subsequent experiments adopted the method of a constant compression of the trachea until lumen occlusion and using the force required for 50% compression as an indicator for the compressive resistance.

It was found that there are multiple factors that affect the mechanical testing results including sample dimensions/size of the indenter, water content in the tissue, and location along the trachea.

Butler et al. find no significant difference between mechanical properties of decellularized human trachea after vacuum decellularization[50]. They performed a larger range of tests – including tensile tests and compression under different orientations – than is presented here, and they find no significant difference compared to native human trachea. Some of the results found in this thesis would also suggest that there is no difference between decellularized porcine trachea and native porcine trachea. However, one thing that Butler et al. note is that the lack of significance may be due to the high variance between samples. Results shown here are in agreement with this.

In one experiment, rings were around 2 cm in width and the indenter used was only 1.25 cm in diameter. This led to edge effects since the compression plate was too small to evenly distribute the load across the trachea. Some rings were compressed unevenly, which produced inaccurate force measures.

To limit edge effects, tracheal rings were cut to 1 cm in width for the next experiment. However, the samples were not kept hydrated in PBS during the sample processing and immediately prior to testing. As a result there may be drying effects that change the mechanical properties since water plays an integral role in the compressive resistance observed in the trachea. Regardless, it is interesting to see that there is an opposing trend for the native vs. decellularized group. It is unclear why this happened, but one hypothesis is that this is a sign of varying protein content based on location in the trachea. Alternatively, the decellularization process may have a varied effect along the length of the trachea.

All previous experiments used different tracheas or different samples within the same trachea for each experimental condition (native vs. decellularized). It was determined that this method is most likely capturing much of the variability between

tracheas rather than the effect of the decellularization process. To account for this, the next experiment involved pairing samples where tracheal rings were tested before and after decellularization and then compared. This should more accurately measure the effect of the decellularization process on the compressive resistance of the tracheal pieces.

The results indicated that the decellularization process does have an effect on the mechanical properties of the trachea. However, it is unclear whether this has a practical effect on the engineered construct. For example, will this change in compressive resistance hinder the ability of epithelial progenitor cells to differentiate into all the cell types of the respiratory epithelium (ciliated cells, goblet cells, etc.)? The results showing the variability of samples within an individual trachea would suggest that the decrease caused by decellularization may not produce a noticeable effect on the final construct. Essentially, the effect caused by decellularization is smaller than the variability already present within the trachea. Indeed, when performing a two-tailed t-test assuming unequal variances for each trachea, trachea 1 ($p=0.180$) and trachea 2 ($p=0.080$) are not statistically significant anymore while trachea 3 ($p=0.0234$) and trachea 4 ($p=0.0055$) still are. This indicates that further testing is required to make a conclusion.

4.2 Sprayer can be used for cell deposition onto multiple substrates without adversely affecting cell viability

Results of preliminary spraying experiments demonstrate that cells can be sprayed without harmful effects on cell viability. There is generally high viability soon after spraying (1 hr to 1 day) with values ranging from 90-98%. These values are much higher than those previously reported. Hendriks et al. looked at optimizing cell viability using a cell spray device (Duploject) that is almost identical – in terms of the aerosolization method – to the one used in this research[51]. They found a viability around 60% using the following parameters: pressure (P) = 0.4×10^5 Pa, nozzle-substrate distance (h) = 3 cm, liquid viscosity (μ) = 1 mPa·s, and a glass substrate. For comparison, typical parameters used in this research were approximately P = 2×10^5 Pa, h = 2 cm, and μ = 1 mPa·s, and multiple types of substrates. These conditions are theoretically much harsher to the cells due to the higher pressure and closer distance of spraying. This translates to smaller droplet sizes and higher impact velocities which are both predicted to have lower viabilities. Additionally, Hendriks et al. posit that poor

outcomes may be unavoidable due to clinical constraints such as the nozzle-substrate distance which may be around 1 cm[51]. The stiffness of the substrate may also be problematic as they found that spraying onto a gelatin surface similar in stiffness to muscle tissue resulted in viabilities close to that of a glass substrate.

Based on the findings in this thesis though, the sprayer device used for this research may be able to overcome these challenges since high viability is maintained at higher pressures, closer distances, and stiffer substrates. This is likely due to an improvement in sprayer nozzle design which can better control droplet size and spray velocity[37,51]. The aerosolization method may also be a factor in the improved cell viability. To produce an aerosol, this device has air traveling through the inner lumen interacting with liquid in the outer lumen. Some devices that have been studied use an opposite configuration with liquid in the inner lumen and air surrounding the liquid[37,52]. Others have also used commercial airbrushes[53] and air-free devices (Penn Century Microsprayer)[54] to aerosolize cells. Ultimately, these factors affect the pressure, shear, and elongational forces that are experienced by cells during spraying and can lead to cell death[40].

4.3 Troubleshooting of HBEC seeding onto trachea

Many experiments were performed to troubleshoot why seeded cells were dying on the decellularized trachea. Ultimately, contamination was found to be the culprit. Still it is useful to discuss the rationale behind the experiments performed to distill some useful information for future research and identify potential pitfalls. There are essentially 5 important parameters to consider when seeding cells onto decellularized tissue: 1) seeding density, 2) media factors for optimal cell survival and differentiation, 3) materials for improved delivery and attachment of cells, 4) residual detergent, and 5) preventing tissue contamination.

Initial seeding experiments had densities of 2.4×10^6, 5×10^5, and 1×10^5 cells/well seeded into tissues on 24-well plates. After cells died, these densities were too high to reasonably expect cells to survive on the tissue based on the size of the tissue (approx. 1 cm^2) and the amount of media available to the cells (approx. 1 mL). Conconi et al. describe using a seeding density of 500,000 cells/cm^2 on decellularized tracheal matrices[55]. If contamination had not been an issue, the second and third experiments may have been optimal in terms of seeding density. Indeed, future experiments of

seeding and spraying were seeded at a range of 100,000 to 500,000 cells/cm^2. Maughan et al. have reported that 1x10^6 cells/cm^2 or greater may be needed for cell seeding in tracheal tissue engineering[56]. Based on these data it would be advisable to run an assay early on with different seeding densities using the cells and tissue that are to be seeded to determine the optimal conditions. Maughan et al. also discuss the potential for reconsidering seeding as a suspension and moving towards cell sheets as a way to improve cell coverage[56]. An alternative to cell sheets is the spray-based delivery system of cells investigated here.

Another idea was to add serum to the media to improve cell viability[57]. The airway epithelial cell media used for seeding experiments is serum-free, which means it does not contain any serum proteins. Serum, commonly in the form of FBS, is added to media during cell culture to provide different growth factors that improve the survival and proliferation of cells. Therefore, adding FBS to the media or incubating the tissue in FBS prior to seeding could improve the outcomes. An alternative to FBS is human platelet lysate which also contains growth factors and proteins for cell culture. It is generally used for culture of MSCs to increase the growth rate and maintain genetic stability of cells. PLTMax, a human platelet lysate, was also used to see if it would provide any improved results. It was interesting to see that incubating the tissues in these reagents led to some slightly improved outcomes, but no significant improvement. This was likely due to short-term effects that improved the environment for HBECs compared to the contaminating organisms.

Cells bind to the ECM through integrins with different integrins binding to different ECM proteins (e.g. $\alpha_5\beta_1$ integrin binds to fibronectin through the RGD sequence)[58,59]. Common ligands for integrins included collagen, fibronectin, and laminin[58,59]. Therefore, coating scaffolds with collagen or fibronectin was thought to improve the attachments of cells to the construct and therefore the survival. This is important to consider when seeding since cell adhesion is critical to seeding outcomes. Use of biomaterials such as fibrin, collagen, and fibronectin has been shown to improve outcomes[35,60–62]. However, this step should only be optimized after it is shown that cells can survive with the tissue being seeded. This approach will be discussed further as a route to clinical application in Section 4.4.

Finally, measuring the residual detergent content in a decellularized tissue can be a relatively simple way to see if detergents are adversely affecting the seeding

process. It was shown by others that a relatively low concentration of detergents is necessary to kill sensitive cells such as HBECs[49]. This emphasizes the importance of properly rinsing decellularized tissue and optimizing a decellularization protocol that works for the tissue of interest.

4.4 Sprayer can be used to deliver bronchial epithelial cells onto decellularized trachea

Multiple experiments showed that HBECs can be successfully delivered onto decellularized trachea scaffolds using a spraying device and cultured up to 9 days. After one day there is approximately 90% viability of HBECs on tracheal samples. At day 3, viability drops to around 80%. Subsequently, though, HBECs appear to grow to confluence at 6 days. This shows that cells are able to proliferate in culture on decellularized tracheal scaffolds after initial cell death caused by spraying.

Many samples have dead cells scattered throughout the surface of the tissue. This is likely due to variability caused by the spraying procedure or culturing of tissues. For example, tissue pieces sprayed near the end of the spraying process may not receive the same number of cells as those at the beginning or middle. Throughout the spraying process, cells may settle inside the syringe leading to a lower concentration that is sprayed. Settling of cells could eventually lead to cell clumping and cell death which would explain that areas of dead cells found on tissues as well. In experiment #2 (Figure 3.21), the sprayer began to produce an abnormal, erratic spray pattern with some of the spray landing outside of the intended wells. This could easily explain why the sprayed tissues at day 8 have many fewer cells compared to the tissues with pipetted cells.

When interpreting the data, a major limitation is that different samples were used for imaging and measurements at different time points. This was done because incubation of cells with LIVE/DEAD stain causes cell death over time. So viability data could not be obtained from the same sample over time. Consequently, variability in the cell spraying procedure from different samples and experiments could cause differences in viability between samples.

It is interesting to note that cells seeded via pipetting or spraying appear to be aligning preferentially along one axis (Figures 3.17 and 3.18). Bronchial epithelial cells do exhibit planar polarity along the longitudinal axis of the trachea which is necessary for proper orientation of the cilia in the mucociliary escalator. This creates a directional

beating of cilia and forces mucus up and out of the airways. If the cells were not polarized in this way, cilia would beat in random directions and potentially produce forces in opposing directions leading to no movement of mucus out of the airways. Since the alignment axis is unknown, it is difficult to assert whether the decellularized matrix, particularly the tunica mucosa and submucosa, are providing topographical cues (i.e. aligned microgrooves on the surface) that produce the observed alignment of the cells. Melo et al. have used this membrane layer as a biotranswell and observed that it leads to a polarized architecture[13]. Although they focused on the apicobasal polarization, it is likely this layer participates in planar polarization as well. This finding warrants further research. If it can be shown that the tunica mucosa and submucosa promote planar polarity it could be a benefit to airway engineering and understanding the polarization of cells.

H&E staining of sprayed samples shows some blue staining in the lacunae of the cartilage which indicates the presence of cellular material. This is somewhat surprising since the trachea has been decellularized prior to spraying so ideally there should not be any cellular content in the scaffold. However, this is consistent with other research showing that some cellular debris is retained inside the cartilage[19,50,55]. It has been described that the tracheal cartilage displays low antigenicity because of the limited blood supply and the dense ECM protecting the chondrocytes[15], so the presence of some cellular material after the decellularization process may be acceptable[11,25]. Additionally, the epithelium is the main site of rejection, thus regenerating an intact epithelium could protect grafts from rejection and reduce immunosuppression[15]. Using multiple decellularization cycles can reduce the amount of DNA content left in the scaffolds; however, the harsh decellularization adversely affects the mechanical properties of the tissue [27]. Therefore, a proper balance has to be maintained to remove enough cellular material to eliminate the possibility of rejection while still preserving the mechanical strength of the tracheal scaffold.

4.5 Considerations for spraying cells in a clinically relevant setting

To show that the cell sprayer could be used in various clinical applications where the tissue topography is not favorable for cell adhesion, cells were sprayed into tracheal ring segments in an upright position. Multiple experiments were performed but it was

difficult to get cells to attach to the scaffolds when spraying in an upright position. These experiments identify considerations and improvements for the spraying process.

One experiment was performed with fibronectin sprayed onto the scaffold as a coating hypothesizing that this would improve cell adhesion. However, this did not improve cell engraftment. The concentration of fibronectin may have to be optimized for there to be a substantial effect on cell adhesion. Use of fibronectin should be studied further since it promotes HBEC adhesion and survival [63]. Other biomaterials such as collagen and laminin are also good candidates for cell delivery. Collagen has been used in a non-spray setting as a matrix to deliver airway cells onto a decellularized tracheal matrix[60]. Laminin is promising since it is the first ECM component that cells encounter when seeded onto a decellularized trachea matrix[13]. Ultimately, the solution may be to use another biomaterial such as fibrin in combination with the cell suspension to spray onto the scaffold. Others have shown that fibrin can be used with a cell spraying device to keep cells stationary immediately after spraying because of its rapid polymerization[31,35–37,40,41]. It is also favorable for regenerative applications since it degrades relatively quickly, so cells can proliferate and differentiate after degradation. Additionally, the cell carrier may provide differentiation cues if stem cells are being used in regeneration[64].

Another concern is the ability for the cell sprayer to deliver high concentration cell suspensions. Throughout multiple spraying experiments the sprayer would become clogged due to clumping of cells. This is a critical shortcoming since large amounts of cells are required to regenerate solid organs such as the lung. Clumping of cells can not only obstruct the sprayer but block smaller airways during recellularization. The current design could affect the ability to spray viscous biomaterials as well. To overcome these challenges, lower cellular concentrations may be used, scaffolds can be sprayed with multiple passes, or the sprayer design would have to be altered.

For clinical translation, the sprayer will likely have to be developed as a single-use device. Currently, the device is manufactured as a custom, handmade product. To move to clinical application, the device will require an automated manufacturing process not only to scale up but to reduce device variability. This would allow for better quality control and standardized device specifications. As mentioned above, small changes in the nozzle design and dimensions can lead to extremely different droplet sizes,

velocities, and forces experienced by cells. Therefore, maintaining uniformity across devices will be key to successful outcomes.

4.6 HBECs maintain at least two epithelial cell markers after spraying

A crucial component of using HBECs for tracheal tissue engineering or airway wound healing is the multipotent capacity of these cells. This means that they can differentiate into ciliated cells and goblet cells of the upper airway. As mentioned in Section 1.1, removal of pathogens from the airway is one of the main functions of the trachea. Thus, having properly functioning ciliated cells and goblet cells is important for an engineered tissue or for repairing an airway injury. To show that HBECs maintain this capacity after spraying and culture, IF staining was performed on sprayed trachea samples. IF staining shows that after culturing sprayed trachea samples for 8 days, HBECs still express CK5 and uteroglobin, which are markers for basal cells and club cells, respectively. This is in agreement with research that shows HBECs express markers of different lung cell types suggesting the potential for differentiation into those cell types[65]. Delgado et al. show that HBECs can display markers of distal lung cells[65].

Unfortunately, the research presented here is unable to definitively show that sprayed HBECs display ciliated cell and goblet cell markers that are most important for the trachea epithelium. Basal cells are thought to be able to differentiate into ciliated cells and goblet cells when necessary, so it is promising that the CK5 marker was found. Additionally, club cells are typically found in more distal parts of the lung such as bronchioles which agrees with Delgado et al. in suggesting that HBECs have larger differentiation capacity than previously thought. From these staining results, it may be reasonable to conclude that the forces experienced by the cells through spraying and the subsequent biological effect do not adversely affect the expression of lung markers. It is yet to be shown that this can translate directly to differentiation capacity.

It is important to remember that these results do not conclusively show that the HBECs are expressing these markers due to being cultured on the decellularized matrix. It is quite possible that these markers are already being expressed during culture in polystyrene flasks and they are just maintained after spraying. One way to determine what is happening would be to perform staining of cells cultured in a chamber slide. Without this information, it is inconclusive one way or the other. Still, this result is

important because it shows at the very least that spraying of HBECs onto decellularized porcine trachea does not negatively affect their epithelial cell marker expression.

5. CONCLUSION

The research presented here focuses on a method for delivering cells to airways using a cell spraying device. To demonstrate the feasibility of the process, HBECs were sprayed onto decellularized porcine trachea. Compressive testing of decellularized porcine trachea was inconclusive, but suggests that some compressive resistance is lost after decellularization. After spraying onto different substrates, HBECs displayed high viability. Sprayed tissues were cultured over one week and the cells retained key epithelial cell markers. This represented the potential for differentiation; however, cells were not definitively differentiated. Cells could not be sprayed in a clinically relevant scaffold setting due to lack of cell attachment.

Overall, results suggest that creation of a tracheal graft or re-epithelialization of airways is achievable, but progress still needs to be made in maintaining differentiating epithelial cells and improving cell attachment. An air-liquid interface culture is likely necessary for differentiation, and cell attachment could be improved by spraying cells within a hydrogel. The success of this method could eventually be translated to whole lung engineering and application of cells to other tissue engineered constructs.

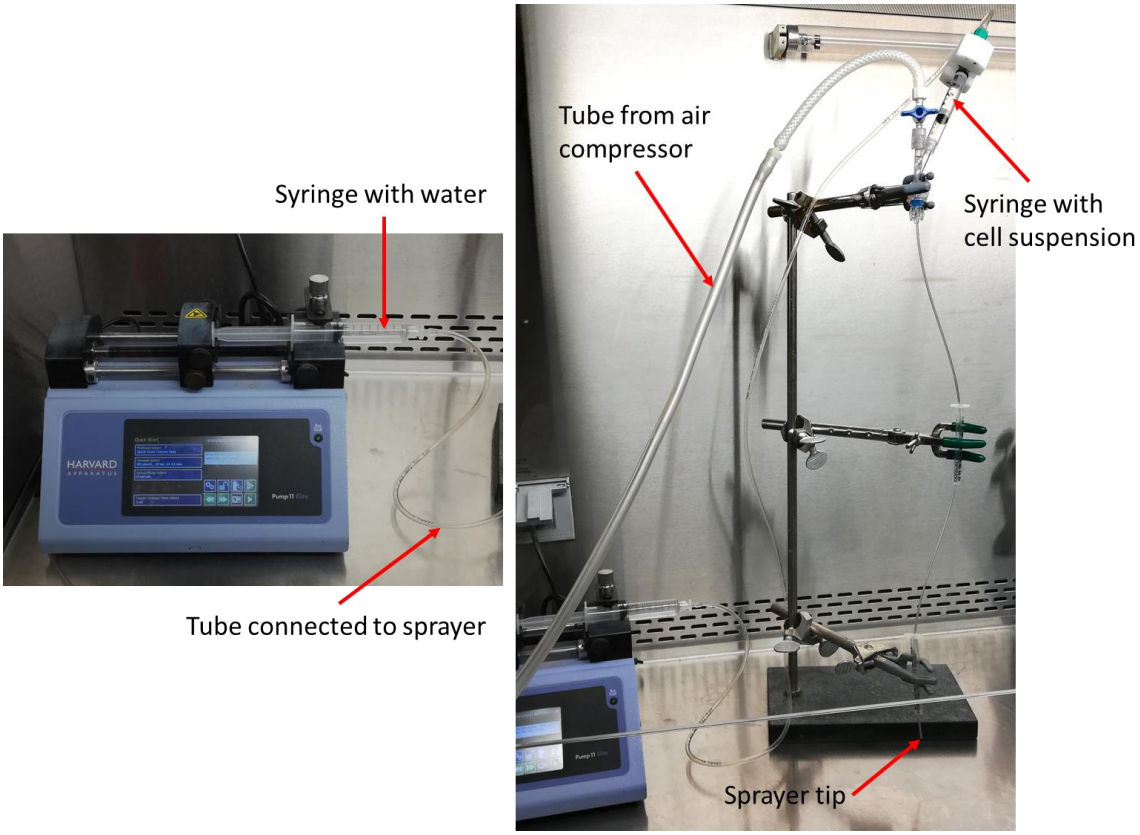

Figure 2.1 – Images of sprayer setup.
Picture of syringe pump with water-filled syringe and tubing connected to sprayer (left). Picture of the sprayer connected to the air compressor tube and the syringe containing cell suspension (right).

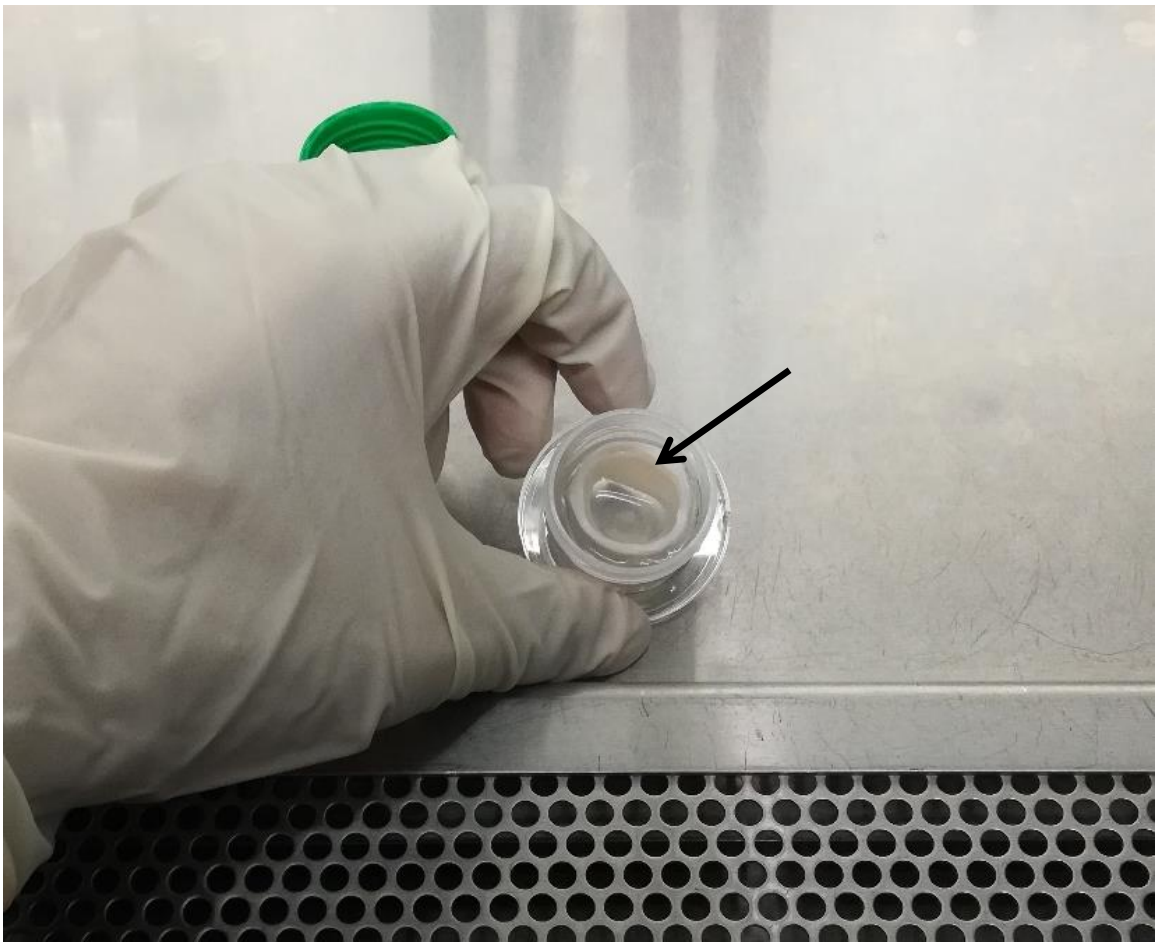

Figure 2.2 – Image of mini-bioreactor setup.
Picture of mini-bioreactor with decellularized trachea (indicated by the solid arrow). Bottom of the bioreactor is filled with 2% agarose to keep the trachea secure.

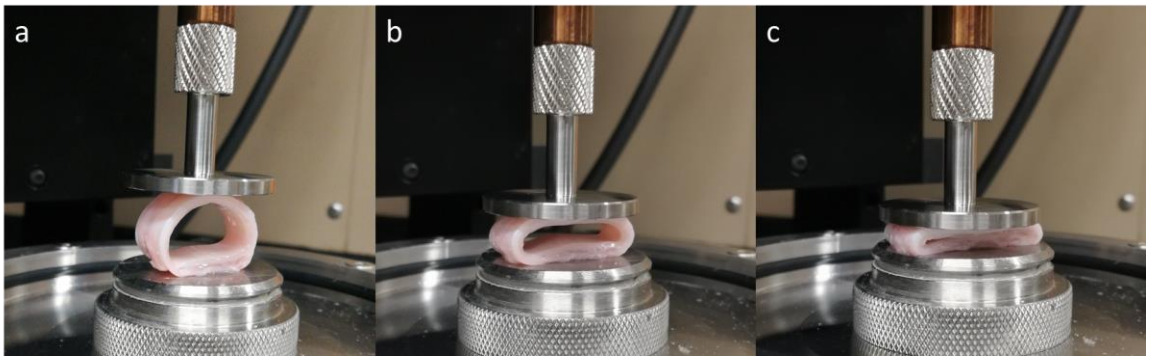

Figure 2.3 – Images of compressive mechanical testing.
Pictures of mechanical testing of native porcine trachea at 3 different stages: (a) no compression, (b) 50% compression, and (c) fully compressed.

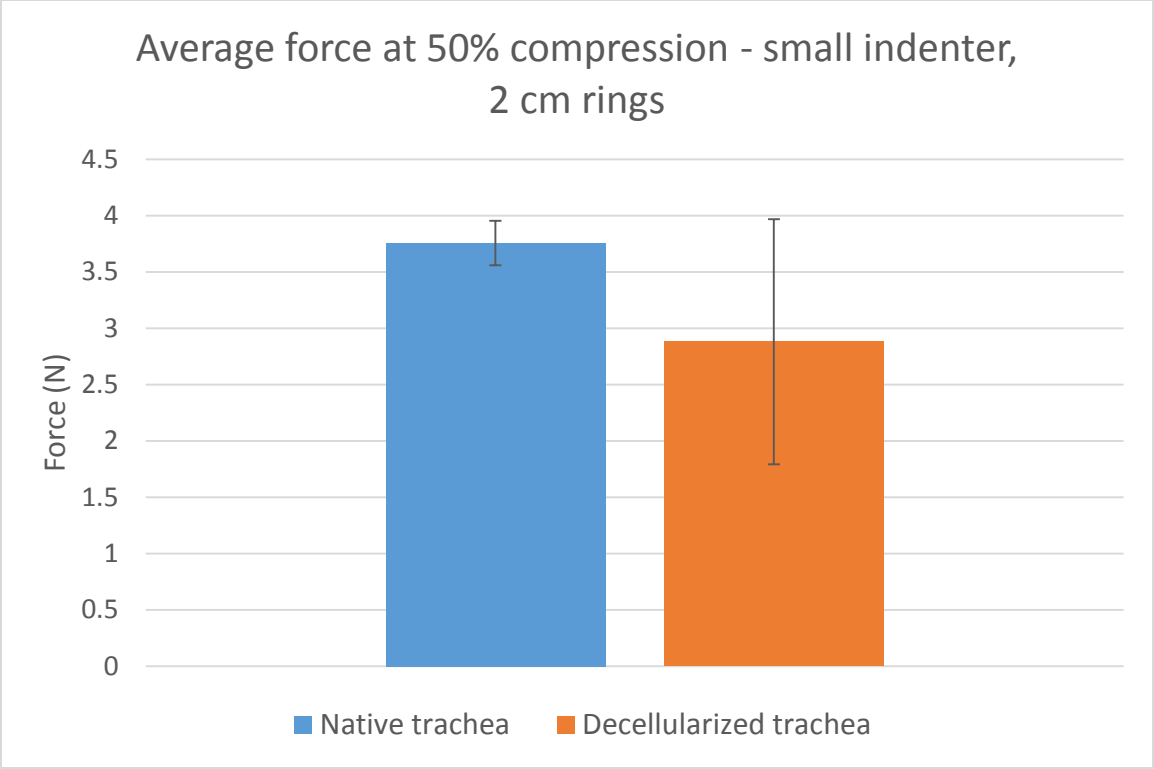

Figure 3.1 – Trachea ring compression with small indenter and 2 cm rings. n=3 for both groups. Testing was performed on one trachea cut into multiple rings (approx. 2 cm in width). Average forces at 50% compression are reported for each group with error bars showing the standard deviation.

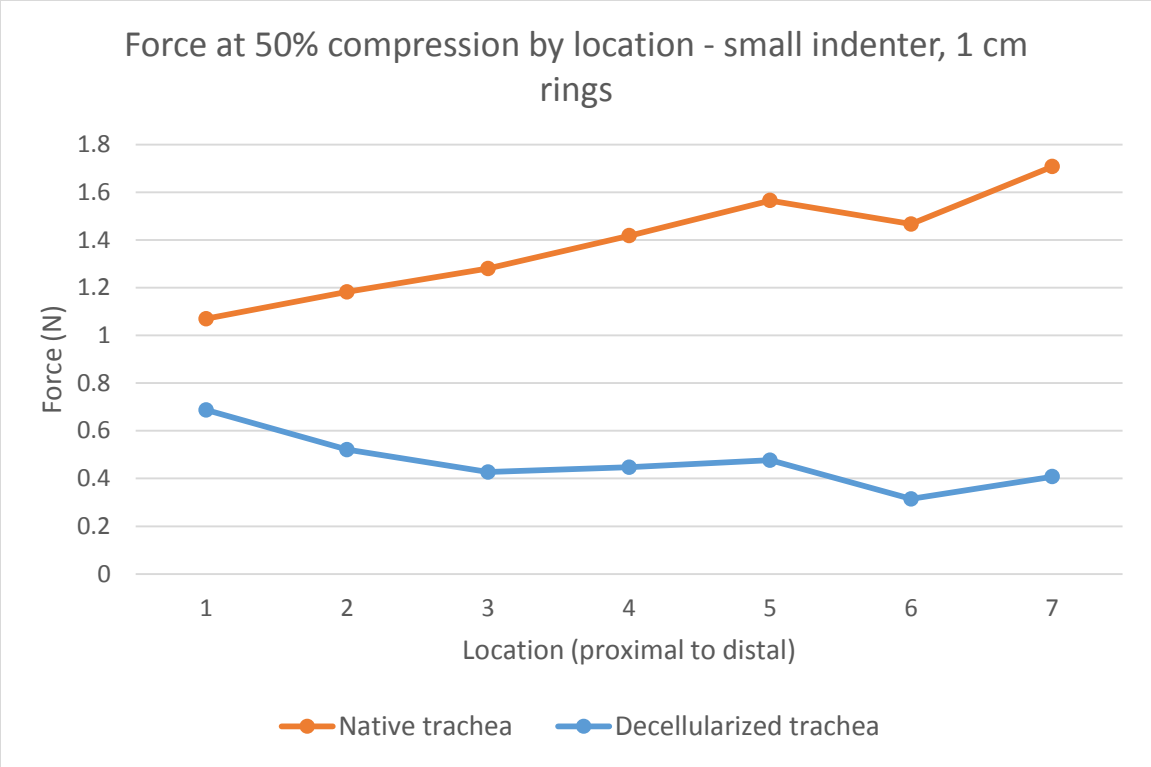

Figure 3.2 – Trachea ring compression by location (proximal to distal) with small indenter and 1 cm rings.
One trachea for each group cut into 7 different rings (approx. 1 cm in width). Samples ordered and tested from proximal (1) to distal (7). Forces at 50% compression are reported for each sample.

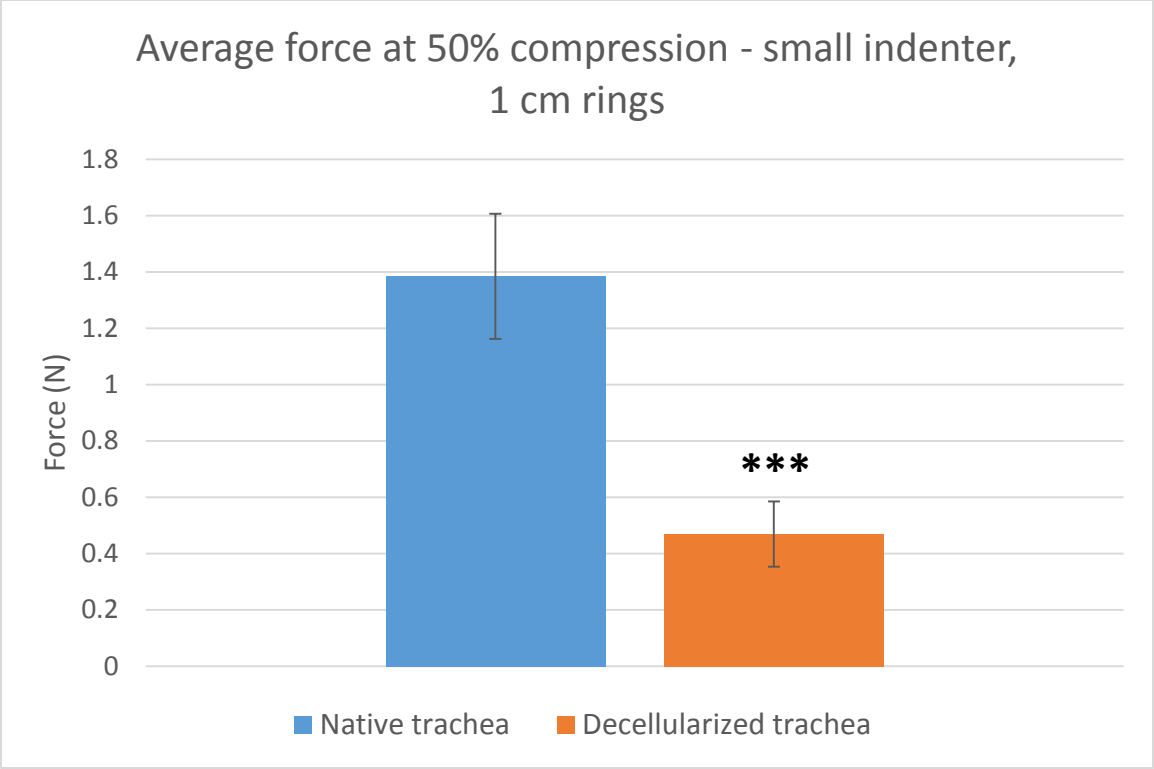

Figure 3.3 – Data from Figure 3.2 averaged by treatment group (native vs. decellularized).
n=7 for both groups. Average forces at 50% compression are reported with error bars showing the standard deviation. Three asterisks indicate statistical significance at the α = 0.001 level ($p=4.7x10^{-6}$). Samples were not paired since a different trachea was tested for each group.

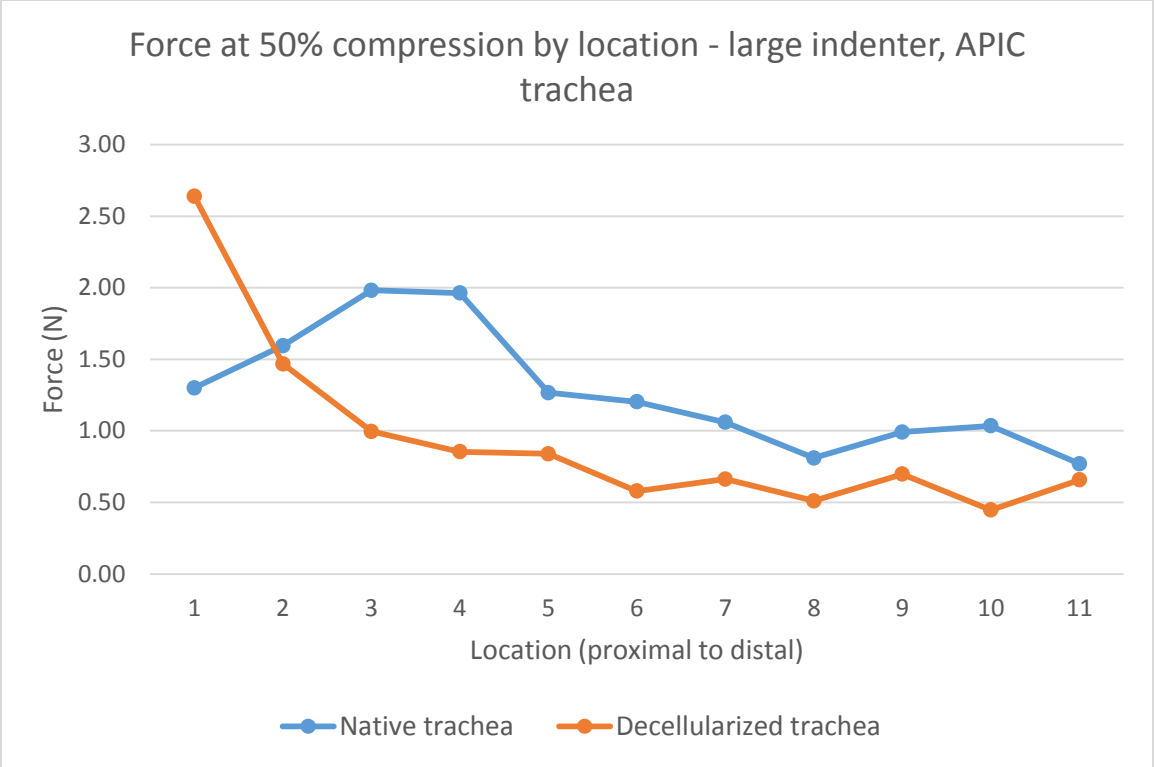

Figure 3.4 – Trachea ring compression by location (proximal to distal) with large indenter and APIC trachea.
One trachea for each group cut into 11 different rings (approx. 1 cm in width). Samples were ordered and tested from proximal (1) to distal (11). Forces at 50% compression are reported for each sample.

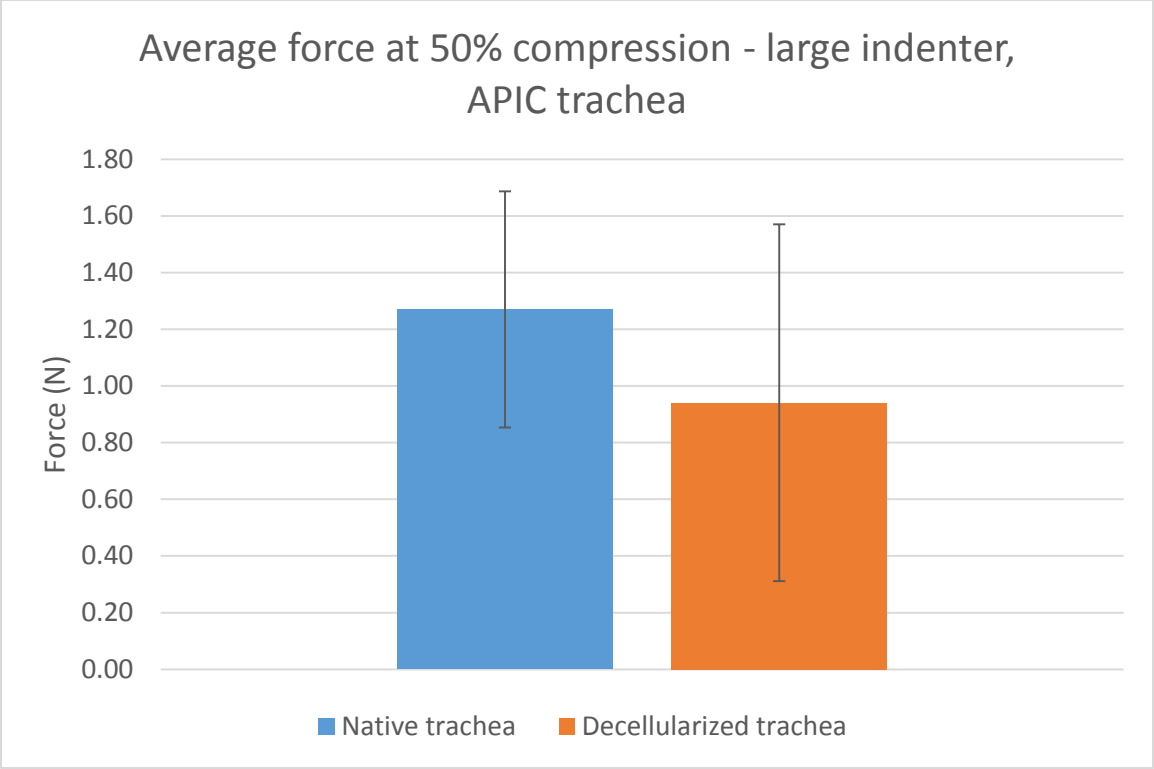

Figure 3.5 – Data from Figure 3.4 averaged by treatment group (native vs. decellularized).
n=11 for both groups. Average forces at 50% compression are reported with error bars showing the standard deviation. There is no statistical significance between the groups and samples were not paired.

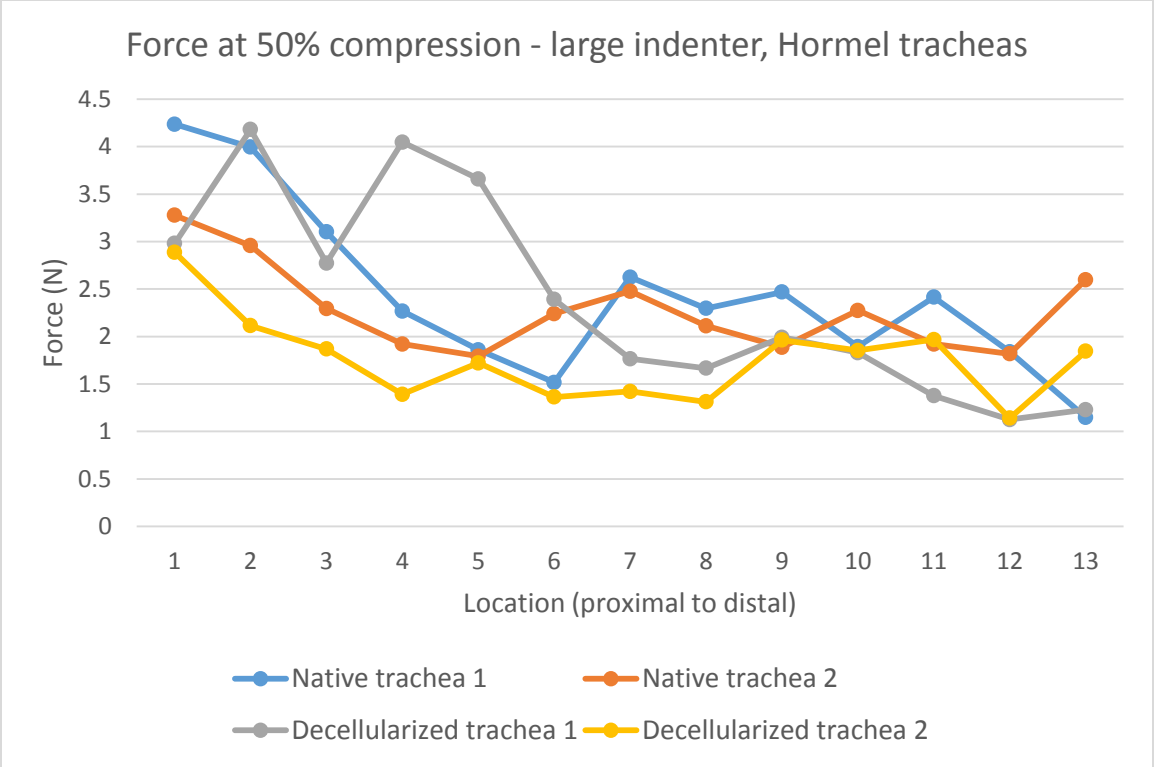

Figure 3.6 – Trachea ring compression by location (proximal to distal) with large indenter and Hormel tracheas.
Two tracheas for each group cut into 13 different samples (approx. 1 cm in width). Samples ordered and tested from proximal (1) to distal (13) or vice versa. Forces at 50% compression are reported for each sample. The variability seen in "Decellularized trachea 1" at location 4 and 5 is likely due to uneven compression where the samples were slanted leading to a higher force than expected.

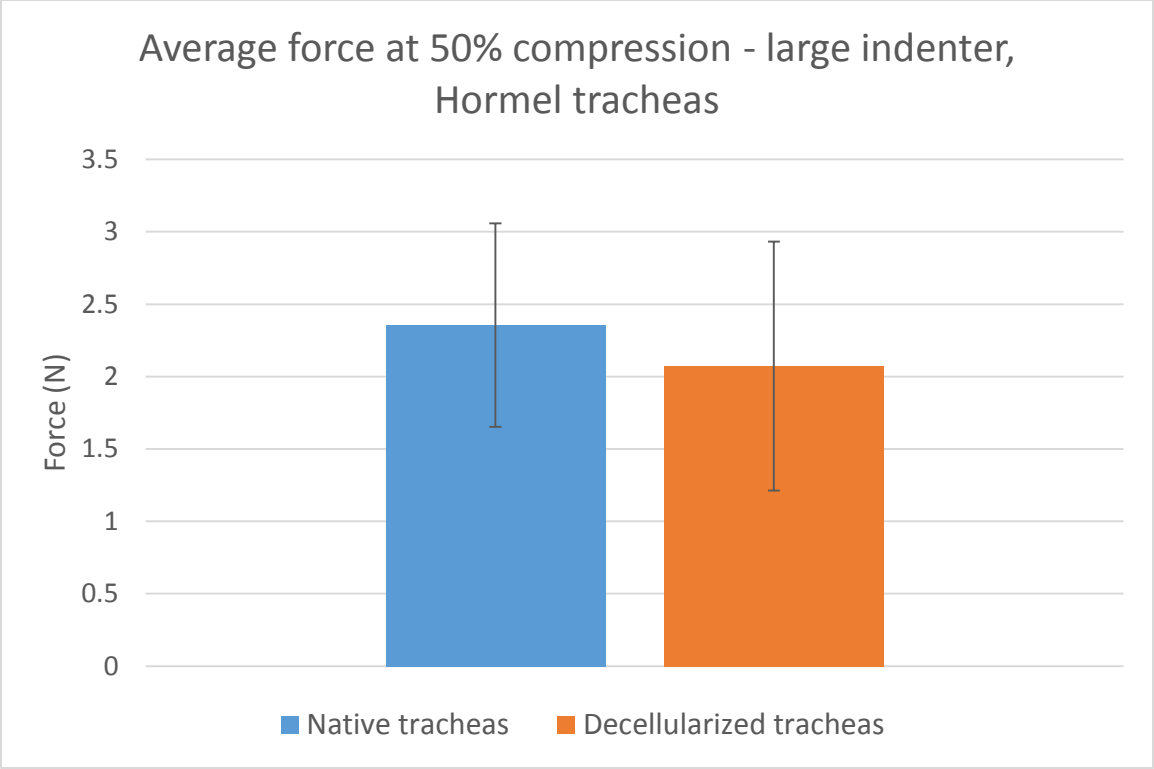

Figure 3.7 – Data from Figure 3.6 averaged by treatment group (native vs. decellularized).
n=26 for both groups. Average forces at 50% compression are reported with error bars showing the standard deviation. There is no significant difference between both groups and samples were not paired.

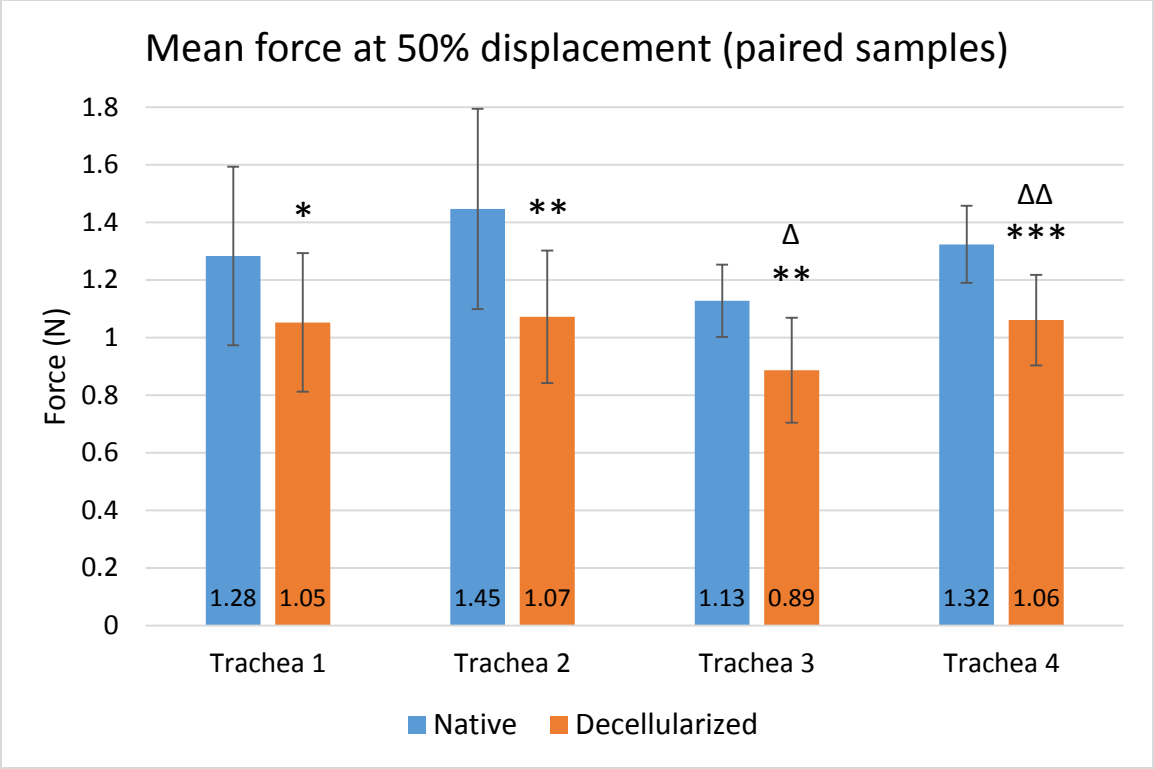

Figure 3.8 – Data from paired samples experiment averaged by treatment group for each trachea.
n=6 for trachea 1 and 3, n=5 for trachea 2, and n=7 for trachea 4. Average forces at 50% compression are reported with error bars showing the standard deviation. Asterisks indicate statistical significance after a paired-sample t-test (* $p<0.05$, ** $p<0.01$, *** $p<0.001$). Triangles indicate statistical significance after a two-tailed t-test assuming unequal variances (Δ $p<0.05$, ΔΔ $p<0.01$).

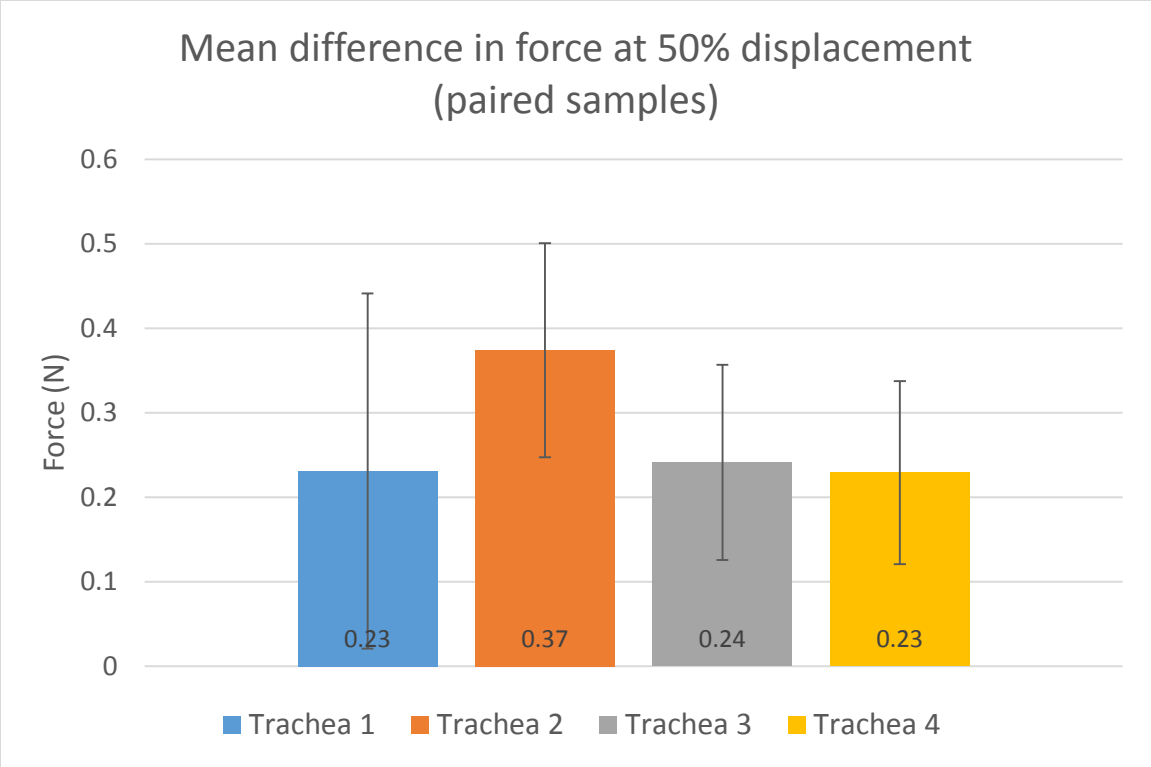

Figure 3.9 – Mean difference in compressive resistance after decellularization. The differences between the forces at 50% compression were calculated for each sample before and after decellularization (difference = native - decell). These differences were then averaged for each trachea and reported here with error bars showing the standard deviations. Positive value indicates that the native samples had a higher force than the decellularized samples.

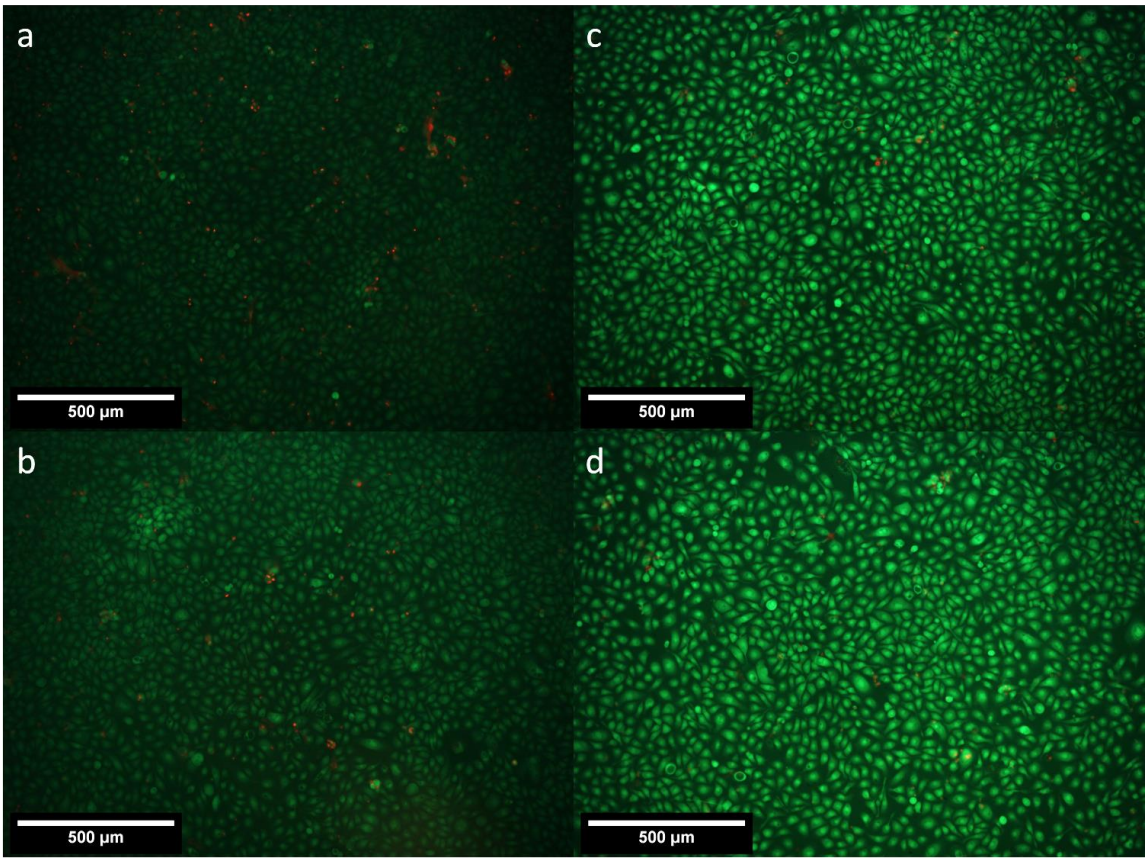

Figure 3.10 – Representative LIVE/DEAD staining images of spraying HBECs into media.
Cells were sprayed at 30 psi and 2 mL/min flow rate. Total volume of 250 uL sprayed and cell concentration of 1 million cells/ml for an approximate seeding density of 250,000 cells/well. HBECs show excellent viability after spraying into media. (a-b) Control condition with cells seeded into an empty well of a 24-well plate via pipetting. (c-d) Representative images of cells sprayed into wells with media. All images are taken 1 day after spraying at 10x magnification.

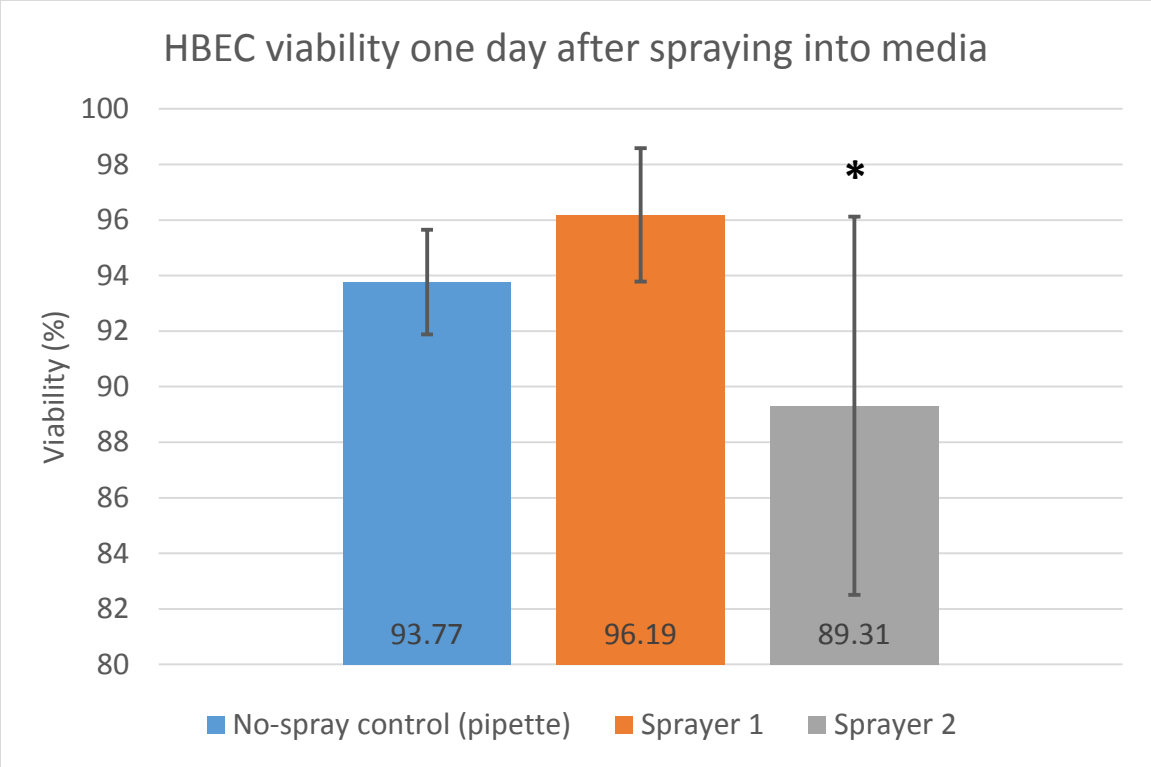

Figure 3.11 – Cell viability one day after spraying into media.
n=3 for the no spray group and n=8 for sprayers 1 and 2. There was an outlier for sprayer 2 around 76% which led to the large deviation. Averages for each group are reported with error bars showing the standard deviation across all the samples in that group. One asterisk indicates statistical significance between Sprayer 2 and Sprayer 1 at the $\alpha = 0.05$ level ($p=0.0295$). Cells were sprayed at 30 psi and 2 mL/min flow rate. Total volume of 250 uL sprayed and cell concentration of 1 million cells/ml for an approximate seeding density of 250,000 cells/well.

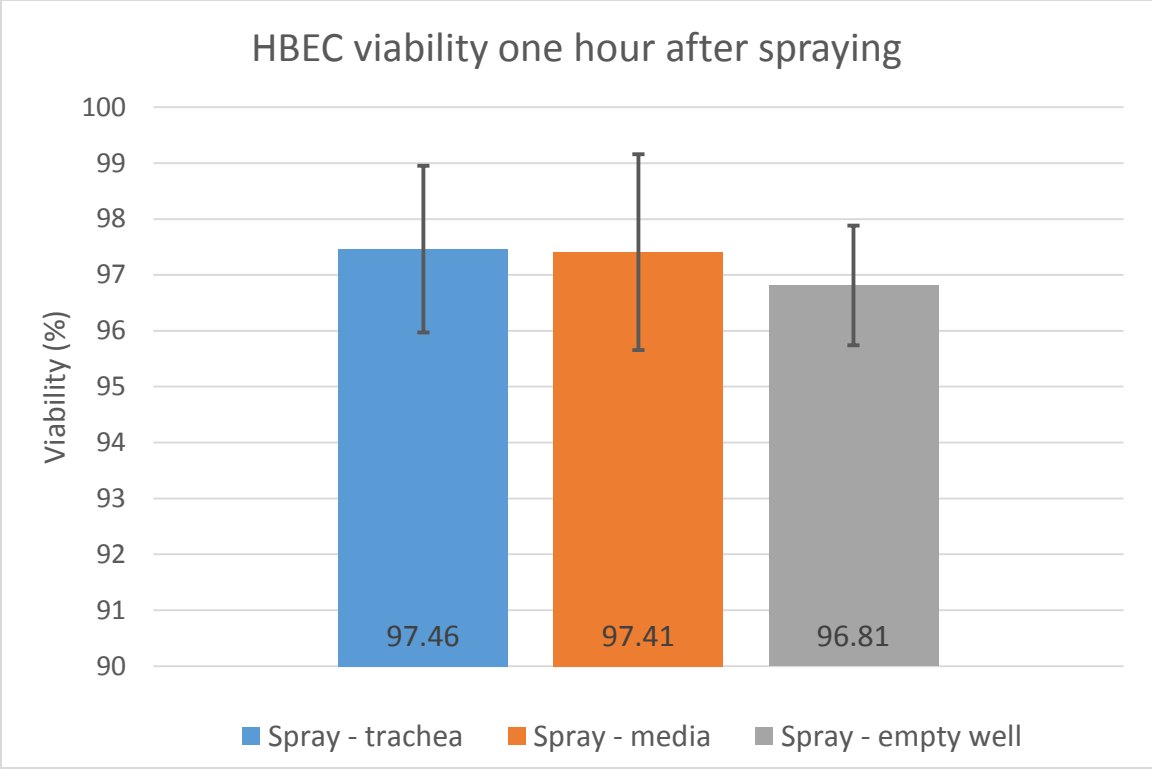

Figure 3.12 – HBEC viability one hour after spraying onto trachea, media, and empty well.
n=3 for each group. Average viability for each group is reported with error bars showing the standard deviation across the samples in that group.

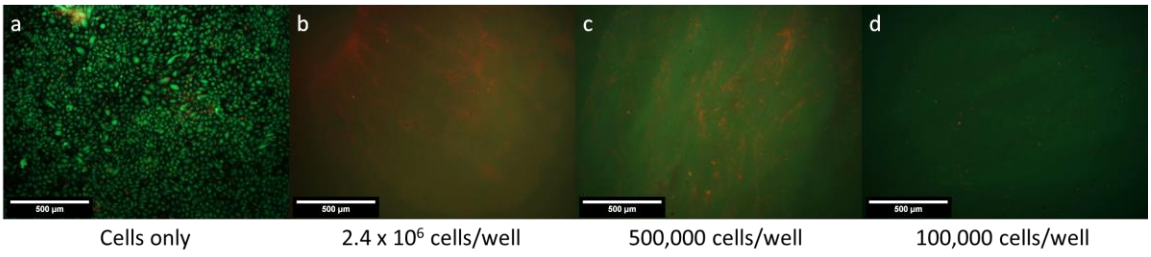

Figure 3.13 – Representative LIVE/DEAD staining images of HBECs pipette-seeded on decellularized trachea pieces at different seeding densities.
(a) Control condition with cells seeded at 100,000 cells/well into an empty well of a 24-well plate. Images of HBECs seeded at different densities – (b) 2.4 x 10^6 cells/well, (c) 500,000 cells/well, and (d) 100,000 cells/well – show no cells on the surface of the tissue. All images are taken 1 day after seeding at 10x magnification.

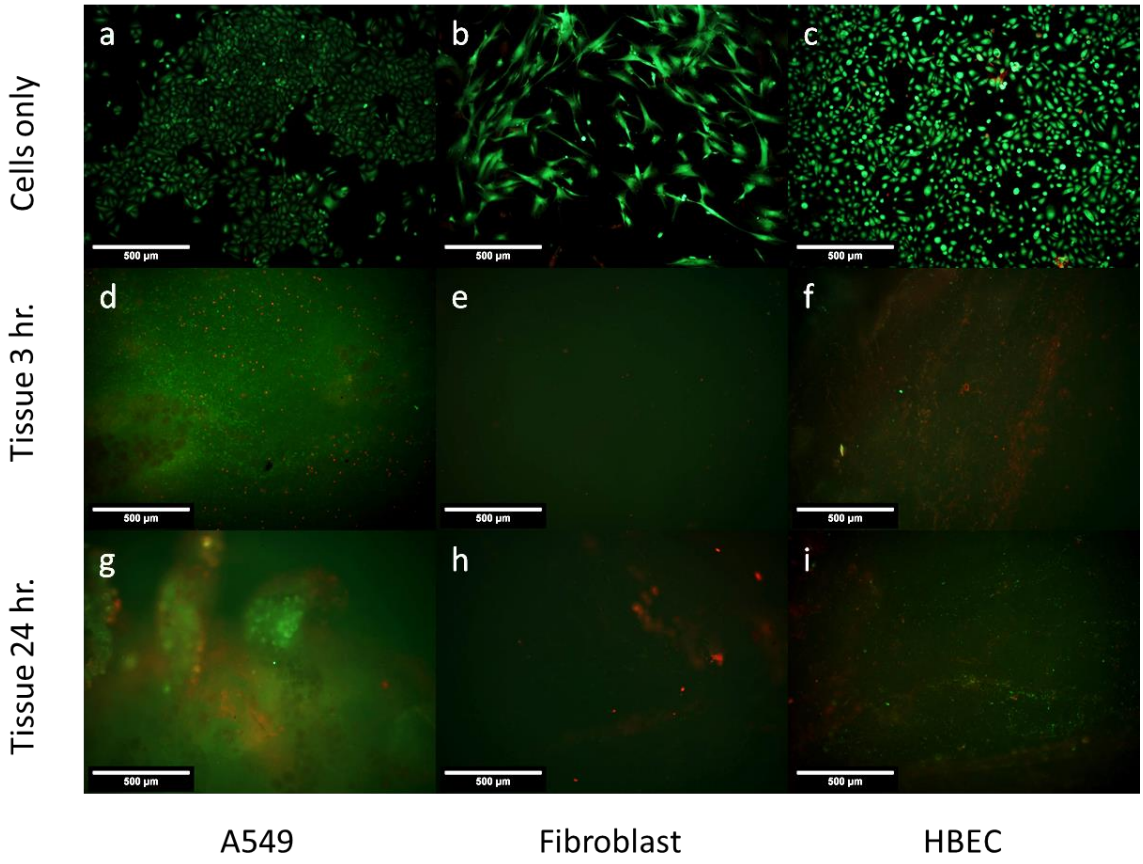

Figure 3.14 – LIVE/DEAD staining images of HBECs, FBs, and A549s pipette-seeded onto decellularized trachea pieces.
(a-c) Control conditions with (a) A549s, (b) FBs, or (c) HBECs seeded into empty wells of a 24-well plate (50,000 cells/well). Tissue samples after 3 hrs seeded with (d) A549s, (e) FBs, or (f) HBECs. Tissue samples after 24 hrs seeded with (g) A549s, (h) FBs, or (i) HBECs. Tissue pieces were soaked overnight in respective culture media prior to seeding with cells. Images are taken 3 hrs and 24 hrs after seeding at 10x magnification.

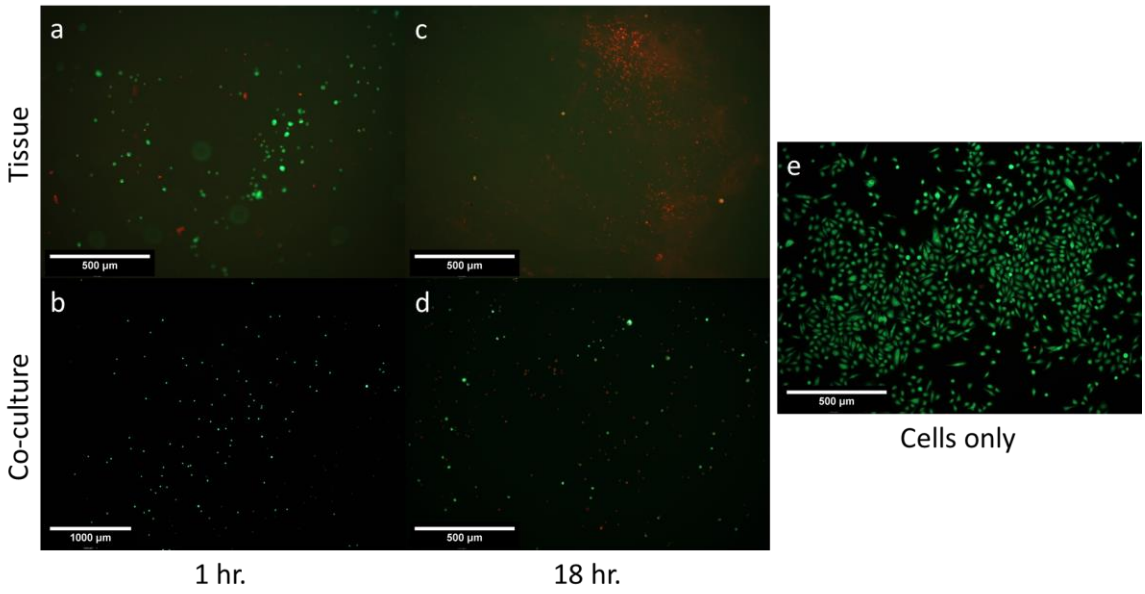

Figure 3.15 – Decellularized trachea seeding and co-culture assay over one day. HBECs were seeded onto decellularized trachea or into a well containing tissue to see whether cell death is due to contact with the tissue or something released by the tissue. Images of HBECs at 1 hr seeded onto trachea (a) or cocultured with trachea (b) and at 18 hrs seeded onto trachea (c) or (d) cocultured with trachea. Image of HBECs for cells-only control (e). Images taken at 10x magnification except for (b) which was taken at 4x magnification.

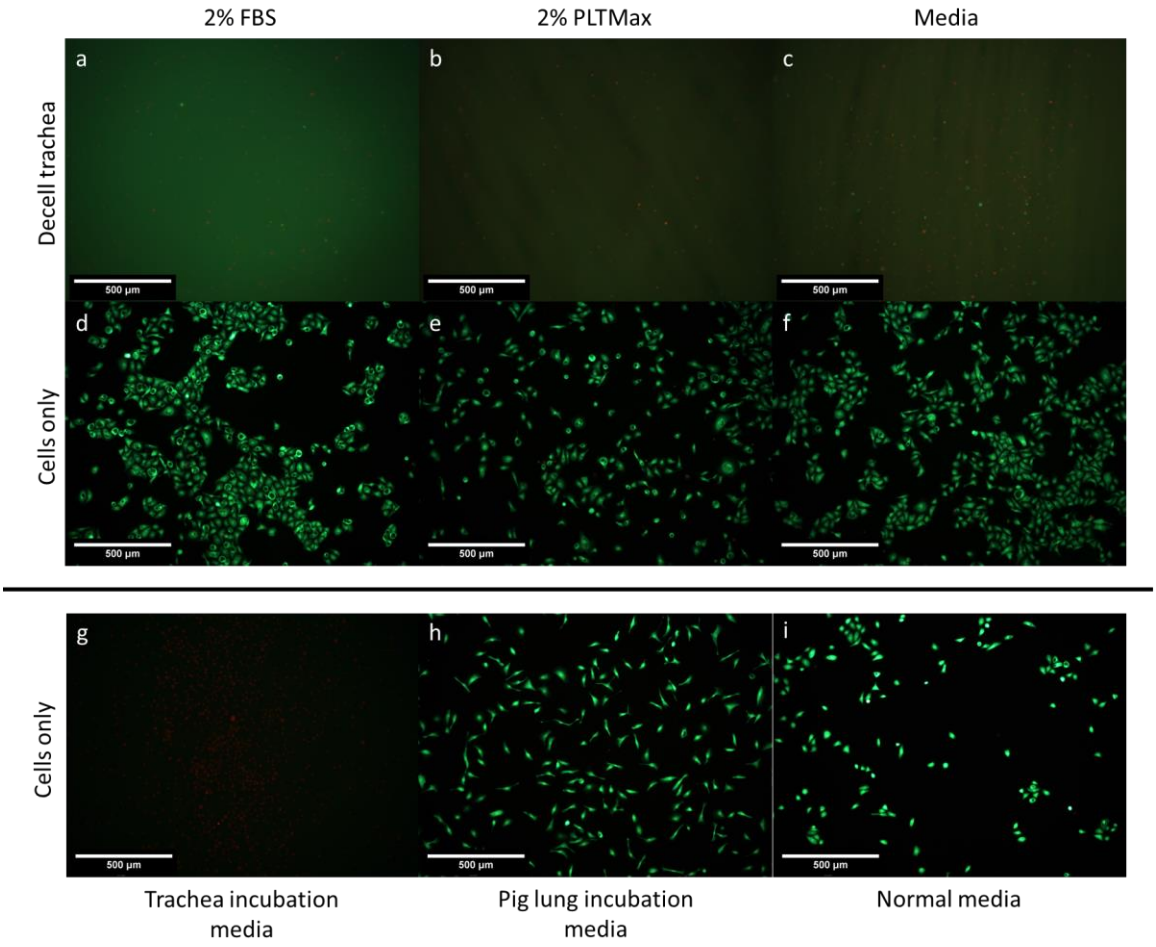

Figure 3.16 – Representative LIVE/DEAD staining images of supplementing media with FBS or PLTMax after seeding and culturing cells in tissue-conditioned media. (a-c) HBECs seeded onto decellularized trachea pieces and cultured with (a) 2% FBS in culture media, (b) 2% PLTMax in culture media, or (c) only culture media. (d-f) Control conditions with HBECs seeded into empty wells of a 24-well plate and cultured with (d) 2% FBS in culture media, (e) 2% PLTMax in culture media, or (f) only culture media. (g-i) HBECs cultured in (g) decell. trachea conditioned media, (h) decell. porcine lung conditioned media, (i) normal cell culture media. All images are taken after 1 day at 10x magnification.

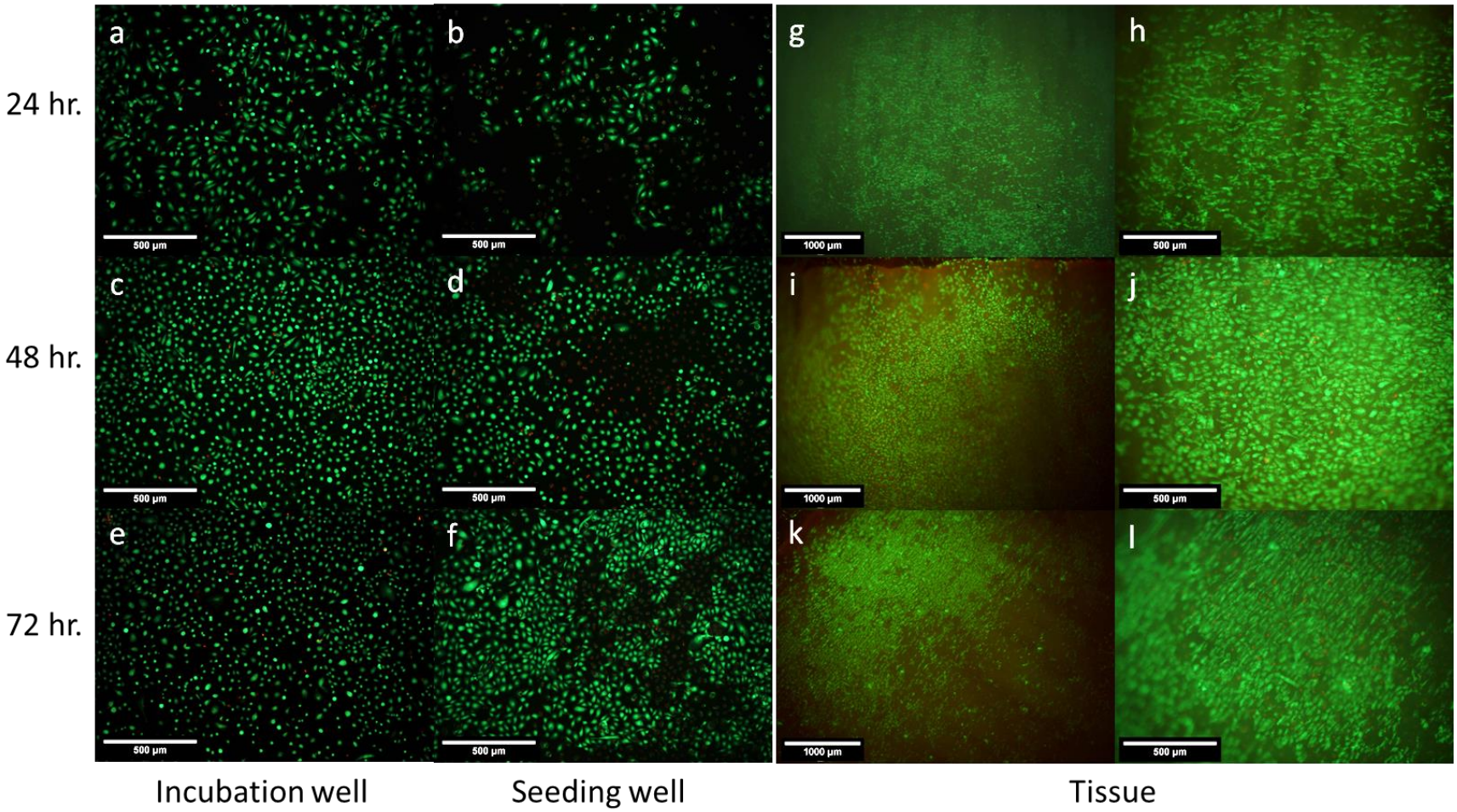

Figure 3.17 – Storing decellularized trachea in pen-strep prior to HBEC seeding via pipetting.
Stored decellularized trachea in pen-strep and incubated tissue pieces in media overnight before seeding via pipetting. Images of HBECs in the incubation well and seeding well at (a-b) 24 hrs, (c-d) 48 hrs, and (e-f) 72 hrs Images of HBECs on decellularized trachea at (g-i) 24 hrs, (j-l) 48 hrs, and (m-o) 72 hrs All images taken at 4x or 10x magnification.

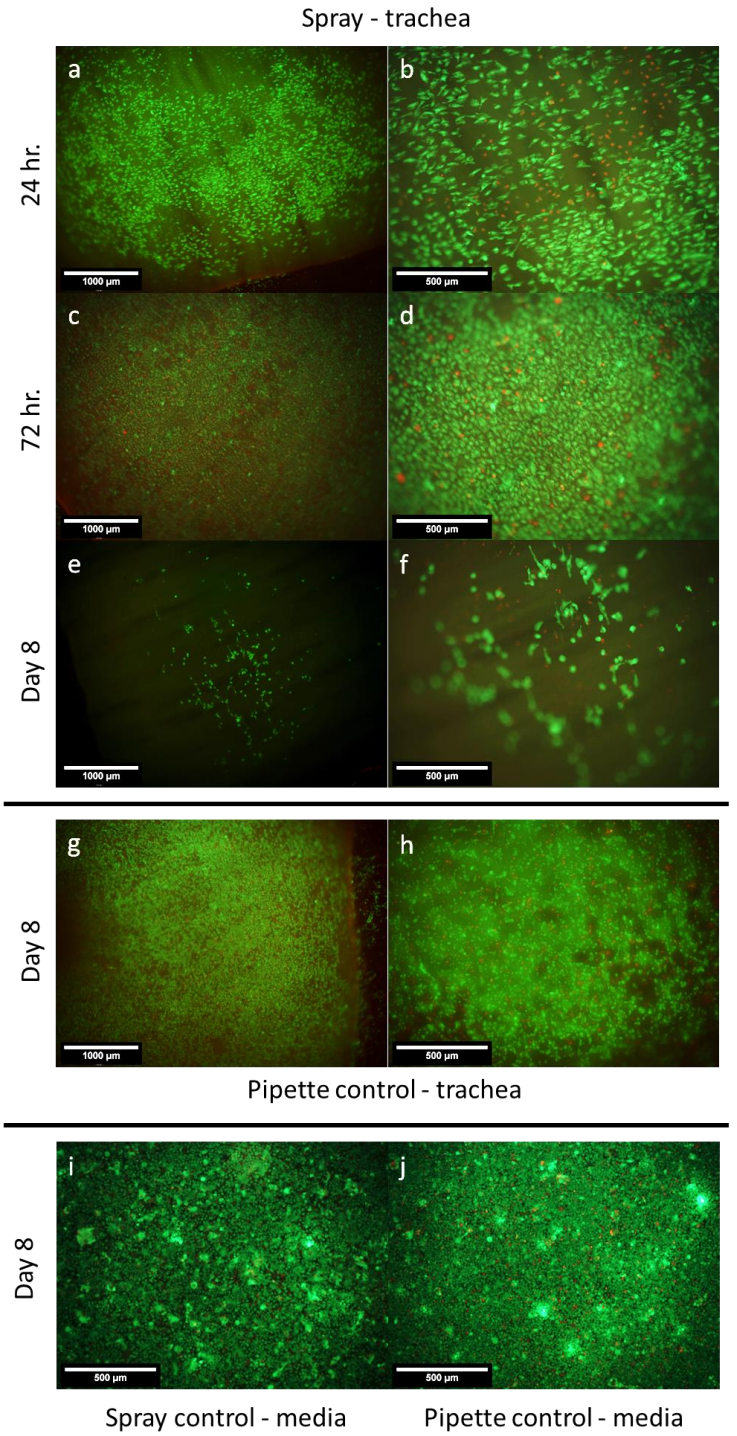

Figure 3.18 – Spraying HBECs onto decellularized trachea pieces (8 day). Tissue was stored in pen-strep after decelling and incubated in media overnight before seeding (250,000 cells/cm^2). Images of HBECs 24 hrs (a-b), 72 hrs (c-d), and 8 days (e-f) after being sprayed onto decellularized trachea pieces in a 24-well plate. Images of HBECs 8 days after being pipetted onto decellularized trachea pieces (g-h) as a control. Images of HBECs 8 days after being sprayed into media (i) or pipetted into media (j) as controls. Images taken at 4x and 10x magnification.

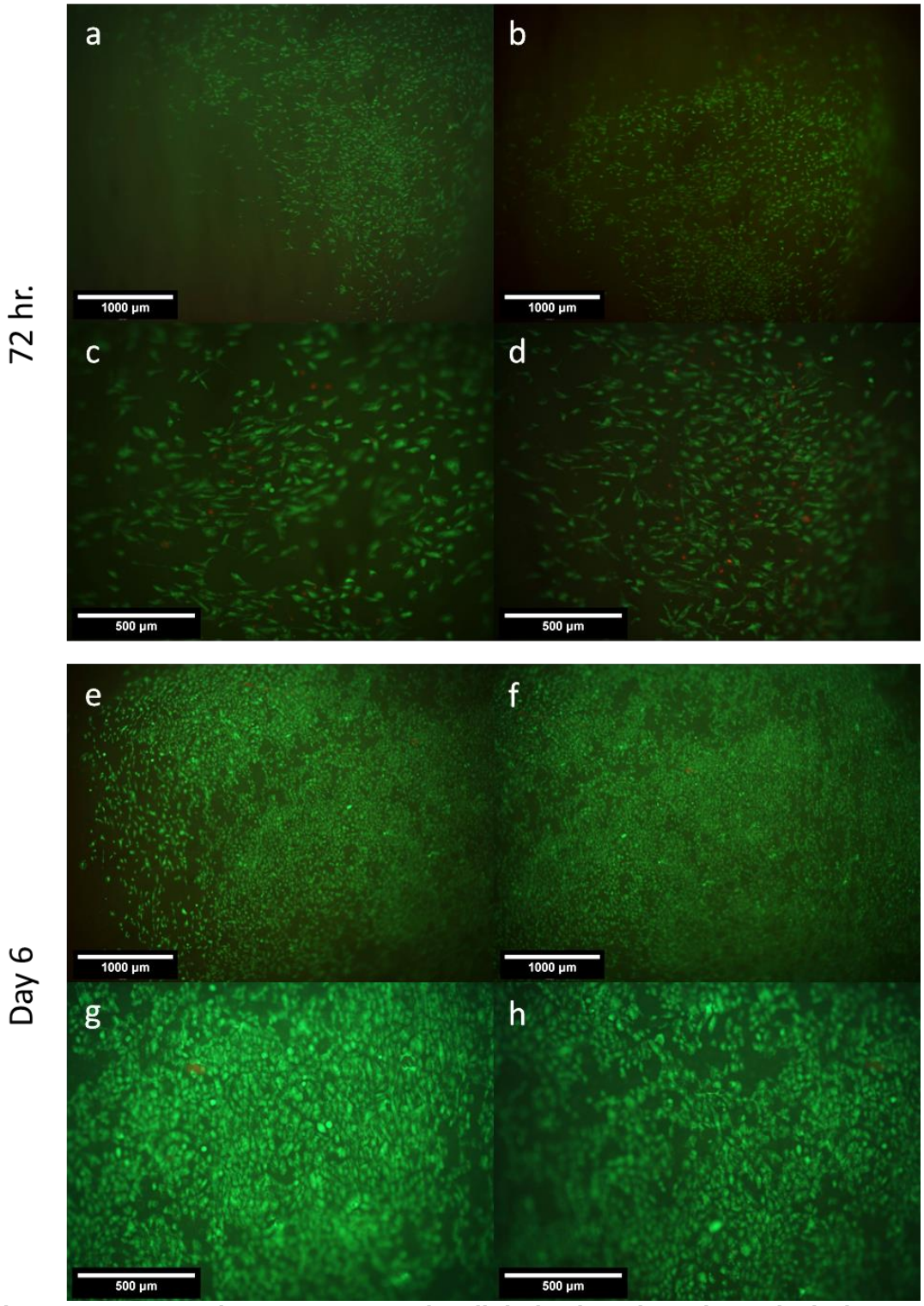

Figure 3.19 – Spraying HBECs onto decellularized trachea pieces (6 day). Tissue was stored in pen-strep after decelling and incubated in media overnight before seeding (80,000 cells/cm^2). Images of HBECs 72 hrs (a-d) and 6 days (e-h) after being sprayed onto decellularized trachea pieces in a 24-well plate. Images taken at 72 hrs and day 6 at 4x and 10x magnification.

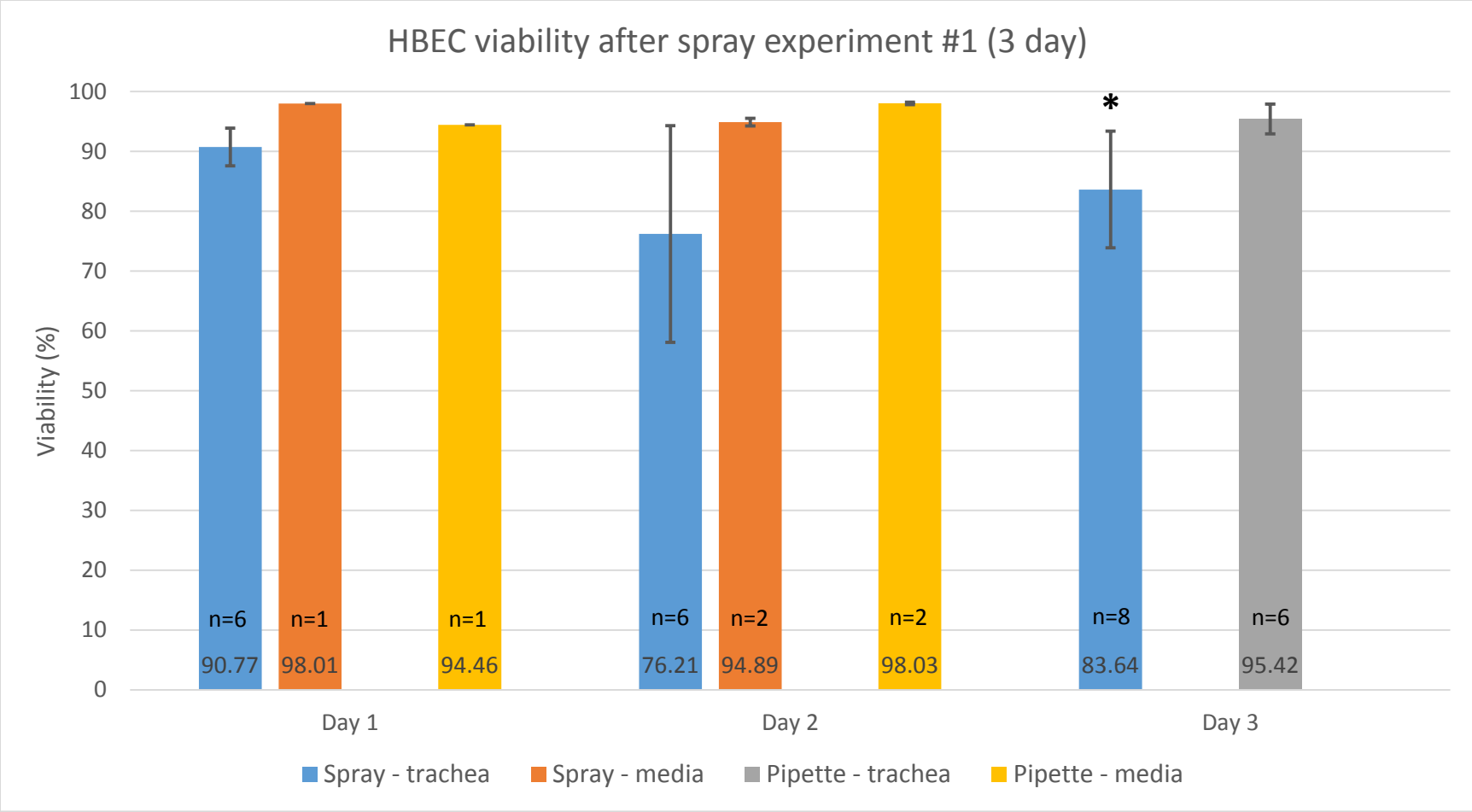

Figure 3.20 – HBEC viability for spray experiment #1 (3 day).
Each bar represents a single sample with *n* technical replicates (images). Average viability of all the images taken from that sample is reported and error bars show the standard deviation of the viabilities within that sample. Asterisk indicates statistical significance between day 3 samples (p=0.0144).

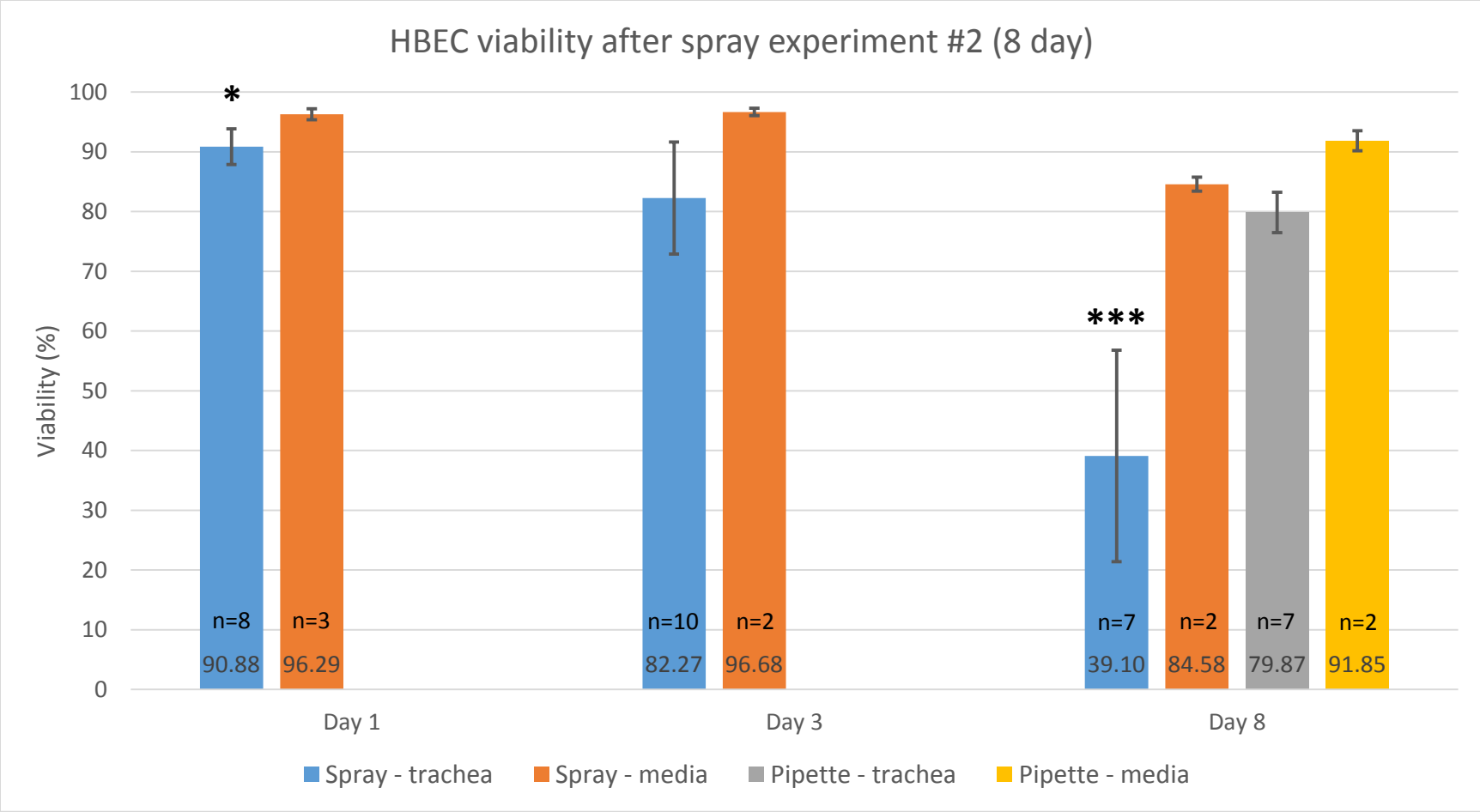

Figure 3.21 – HBEC viability for spray experiment #2 (8 day).
Each bar represents a single sample with *n* technical replicates (images). Average viability of all the images taken from that sample is reported and error bars show the standard deviation of the viabilities within that sample. One asterisk indicates statistical significance at α = 0.05 level between day 1 samples. Three asterisks indicate statistical significance at the α = 0.001 level between day 8 samples.

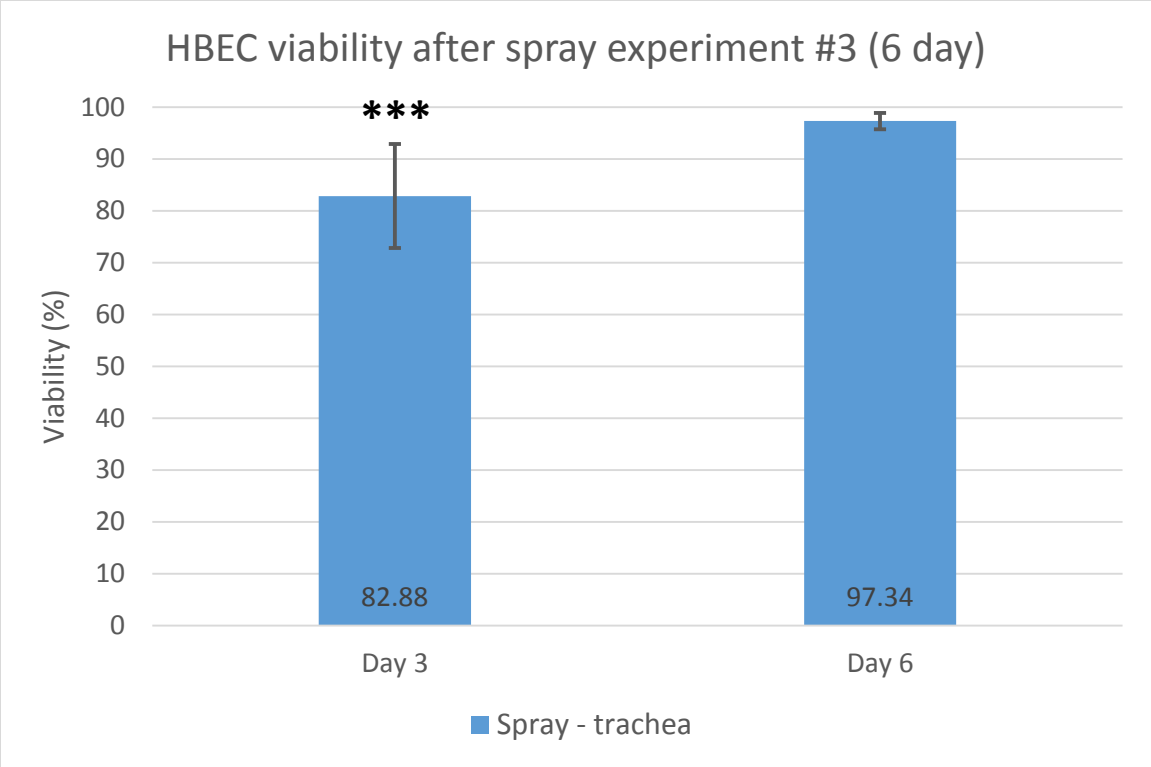

Figure 3.22 – HBEC viability for spray experiment #3 (6 day).
n=3 for each group. Average viability for each group is reported with error bars showing the standard deviation across the samples in that group. Three asterisks indicate statistical significance at the α = 0.001 level between day 8 samples. The increased viability seen at Day 6 suggests that cells can proliferate after spraying to cover the surface of the tissue.

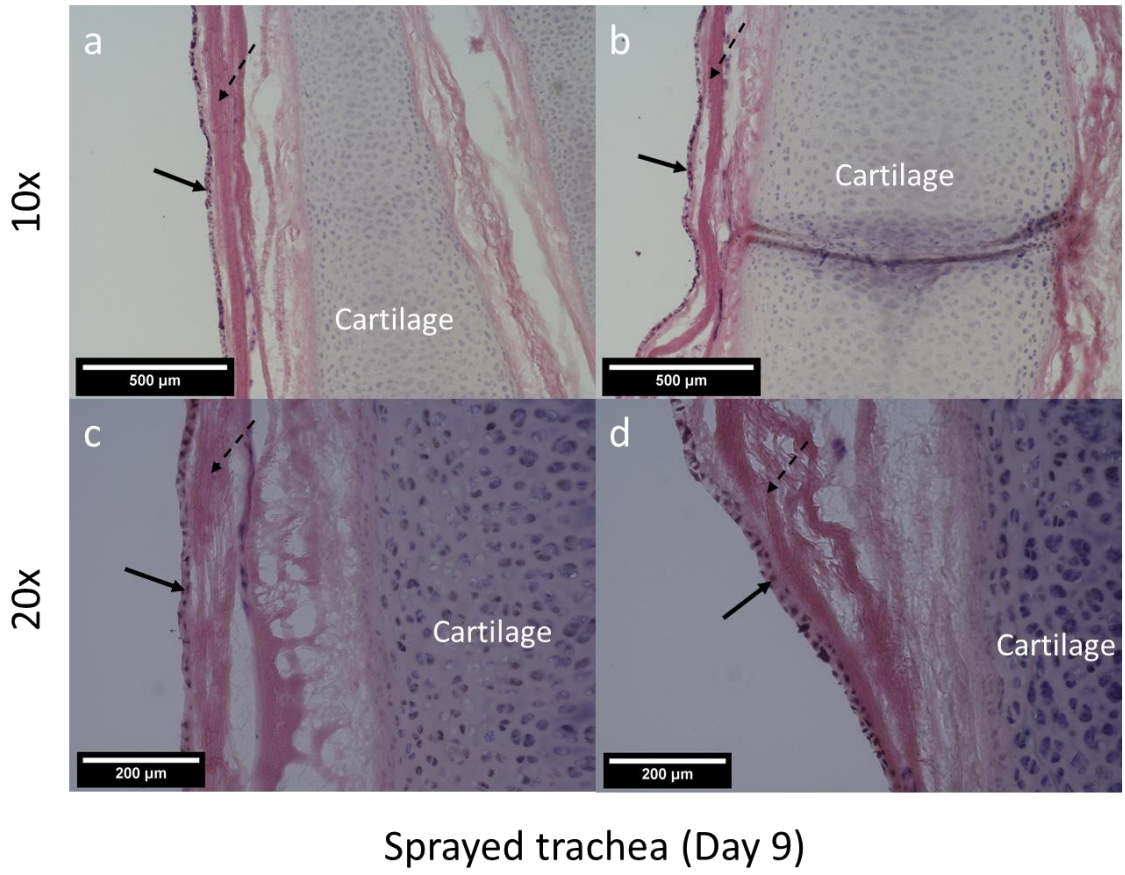

Figure 3.23 – Representative H&E staining images of sprayed trachea samples at day 9.
Images at 10x (a-b) and 20x (c-d). Solid arrows indicate HBECs, dashed arrows indicate the epithelial membrane, and cartilage is labeled with text. Images (a-b) are from a different experiment than images (c-d). H&E shows good coverage of epithelial layer at day 9.

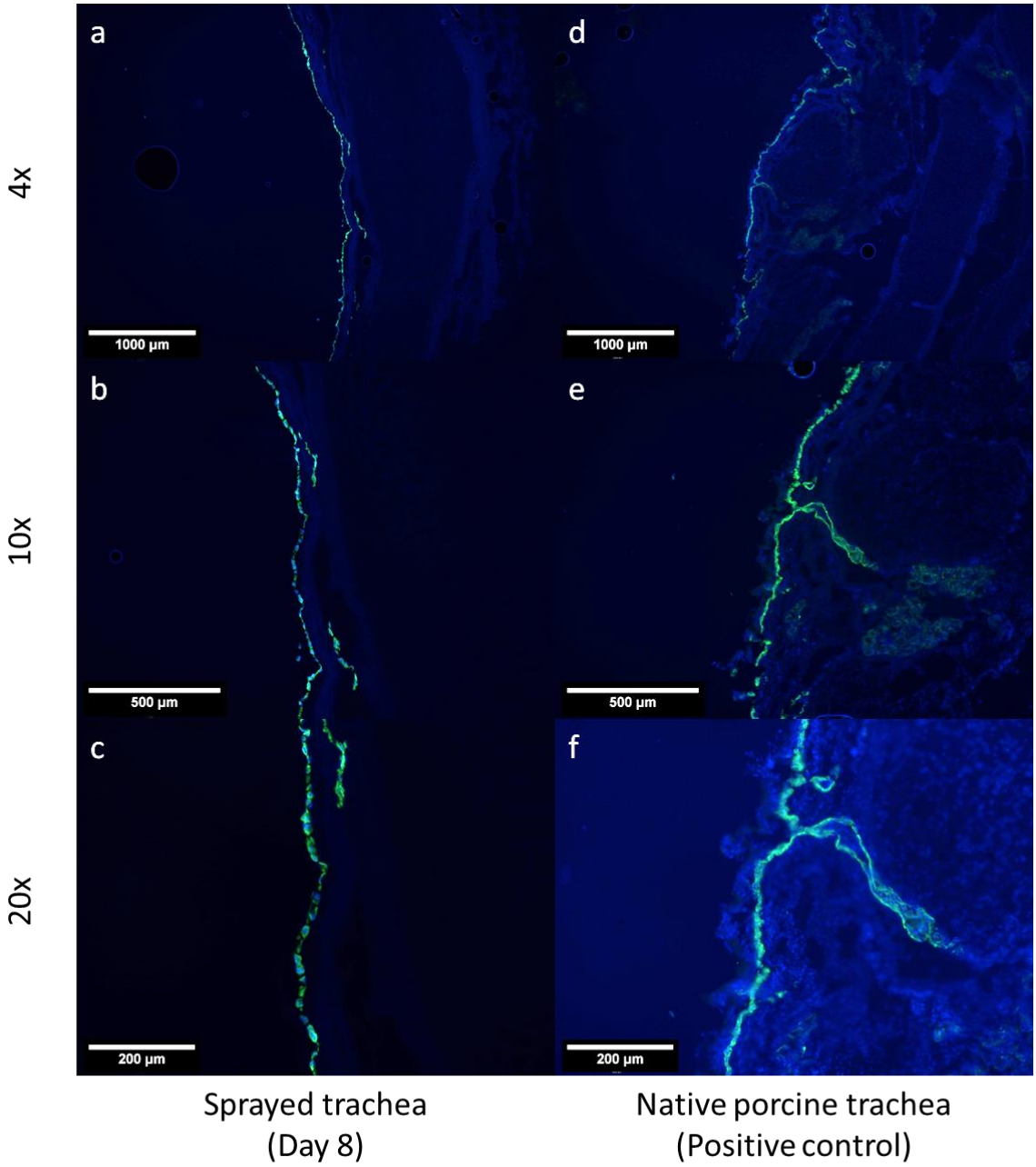

Figure 3.24 – Representative CK5 immunofluorescent staining images of sprayed trachea samples at day 8.
Images at 4x (a,d), 10x (b,e) and 20x (c,f). Images of sprayed trachea sample at day 8 (a-c) and native porcine trachea used as a positive control (d-f). HBECs show excellent staining for CK5, which is similar to the positive control.

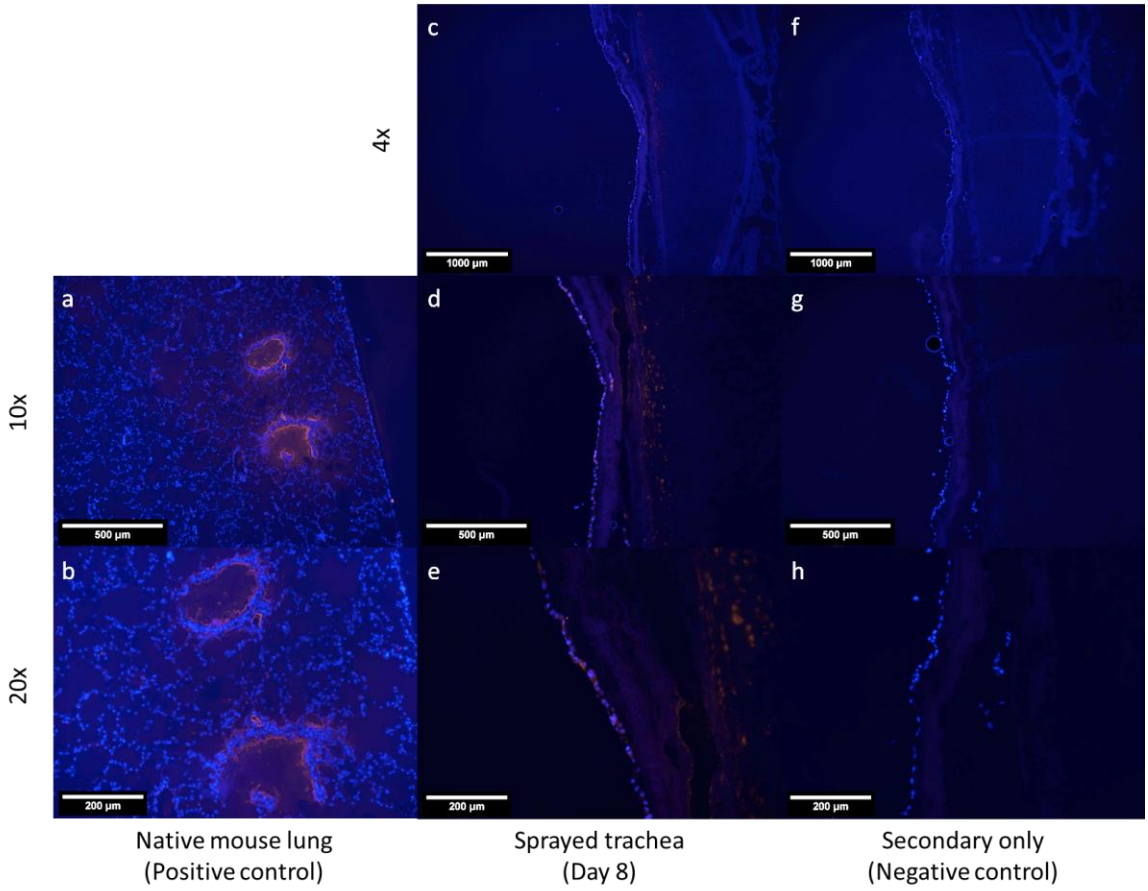

Figure 3.25 – Representative uteroglobin immunofluorescent staining images of sprayed trachea samples at day 8.
Images of native mouse lung used as positive control (a-b), sprayed trachea sample at day 8 (c-e), and samples with secondary antibody only as negative control (f-h). Images at 4x (c,f), 10x (a,d,g) and 20x (b,e,h). HBECs show diffuse staining that is similar to the positive control and not seen in the negative control.

6. Bibliography

1. Furlow, P. W. & Mathisen, D. J. Surgical anatomy of the trachea. *Ann. Cardiothorac. Surg.* **7**, 255–260 (2018).
2. Udelsman, B., Mathisen, D. J. & Ott, H. C. A reassessment of tracheal substitutes—a systematic review. *Ann. Cardiothorac. Surg.* **7**, 175–182 (2018).
3. Haykal, S., Salna, M., Waddell, T. K. & Hofer, S. O. Advances in Tracheal Reconstruction. *Plast. Reconstr. Surg. Glob. Open* **2**, 1–11 (2014).
4. Boazak, E. M. & Auguste, D. T. Trachea Mechanics for Tissue Engineering Design. *ACS Biomater. Sci. Eng.* **4**, 1272–1284 (2018).
5. Roberts, C. R. *et al.* Ultrastructure and tensile properties of human tracheal cartilage. *J. Biomech.* **31**, 81–86 (1998).
6. Roughley, P. J. & Lee, E. R. Cartilage proteoglycans: Structure and potential functions. *Microsc. Res. Tech.* **28**, 385–397 (1994).
7. Safshekan, F., Tafazzoli-Shadpour, M., Abdouss, M. & Shadmehr, M. B. Viscoelastic Properties of Human Tracheal Tissues. *J. Biomech. Eng.* **139**, 011007 (2017).
8. Salassa, J. R., Pearson, B. W. & Spencer, W. Gross and Microscopical Blood Supply of the Trachea. *Ann. Thorac. Surg.* **24**, 100–107 (1977).
9. Zhang, H., Fu, W. & Xu, Z. Re-epithelialization: A key element in tracheal tissue engineering. *Regen. Med.* **10**, 1005–1023 (2015).
10. Delaere, P. & Raemdonck, D. Van. Tracheal replacement. *J. Thorac. Dis.* **8**, S186–S196 (2016).
11. Balestrini, J. L. & Niklason, L. E. Extracellular Matrix as a Driver for Lung Regeneration. *Ann. Biomed. Eng.* **43**, 568–576 (2015).
12. Orlando, G., Soker, S. & Stratta, R. J. Organ bioengineering and regeneration as the new holy grail for organ transplantation. *Ann. Surg.* **258**, 221–232 (2013).
13. Melo, E., Kasper, J. Y., Unger, R. E., Farré, R. & Kirkpatrick, C. J. Development of a Bronchial Wall Model: Triple Culture on a Decellularized Porcine Trachea. *Tissue Eng. Part C Methods* **21**, 909–921 (2015).
14. Gilpin, S. E. & Wagner, D. E. Acellular human lung scaffolds to model lung disease and tissue regeneration. *Eur. Respir. Rev.* **27**, 180021 (2018).
15. Delaere, P. R. Tracheal transplantation. *Curr. Opin. Pulm. Med.* **18**, 313–320 (2012).
16. Ott, L. M., Weatherly, R. A. & Detamore, M. S. Overview of tracheal tissue engineering: Clinical need drives the laboratory approach. *Ann. Biomed. Eng.* **39**, 2091–2113 (2011).
17. Kojima, K. & Vacanti, C. A. Tissue Engineering in the Trachea. *Anat. Rec.* **297**, 44–50 (2014).
18. Carden, K. A., Boiselle, P. M., Waltz, D. A. & Ernst, A. Tracheomalacia and tracheobronchomalacia in children and adults: An in-depth review. *Chest* **127**, 984–1005 (2005).
19. Zang, M., Zhang, Q., Chang, E. I., Mathur, A. B. & Yu, P. Decellularized tracheal matrix scaffold for tissue engineering. *Plast. Reconstr. Surg.* **130**, 532–540 (2012).
20. Haykal, S., Salna, M. & Waddell, T. K. Reconstructive Advances in Tracheal Reconstruction. 1–11 doi:10.1097/GOX.0000000000000097
21. Badylak, S. F., Freytes, D. O. & Gilbert, T. W. Extracellular matrix as a biological scaffold material: Structure and function. *Acta Biomater.* **5**, 1–13 (2009).
22. Hryhorowicz, M., Zeyland, J., Słomski, R. & Lipiński, D. Genetically Modified Pigs

as Organ Donors for Xenotransplantation. *Mol. Biotechnol.* **59**, 435–444 (2017).
23. Cooper, D. K. C. *et al.* Xenotransplantation - The current status and prospects. *Br. Med. Bull.* **125**, 5–14 (2018).
24. Cooper, D. K. C., Ekser, B., Ramsoondar, J., Phelps, C. & Ayares, D. The role of genetically engineered pigs in xenotransplantation research. *J. Pathol.* **238**, 288–299 (2016).
25. Tsuchiya, T. *et al.* Future prospects for tissue engineered lung transplantation. *Organogenesis* **10**, 196–207 (2014).
26. Cooper, D. K. C. & Bottino, R. Recent Advances in Understanding Xenotransplantation: Implications for the Clinic. *Expert Rev Clin Immunol.* **11**, 1379–1390 (2015).
27. Keane, T. J., Swinehart, I. T. & Badylak, S. F. Methods of tissue decellularization used for preparation of biologic scaffolds and in vivo relevance. *Methods* **84**, 25–34 (2015).
28. Crapo, P. M., Gilbert, T. W. & Badylak, S. F. An overview of tissue and whole organ decellularization processes. *Biomaterials* **32**, 3233–3243 (2011).
29. Galliger, Z. & Panoskaltsis-Mortari, A. Tracheal Cartilage Isolation and Decellularization. *Methods Mol. Biol.* 155–160 (2018). doi:10.1007/7651
30. Schwartz, D. M., Pehlivaner Kara, M. O., Goldstein, A. M., Ott, H. C. & Ekenseair, A. K. Spray Delivery of Intestinal Organoids to Reconstitute Epithelium on Decellularized Native Extracellular Matrix. *Tissue Eng. Part C Methods* **23**, 565–573 (2017).
31. ter Horst, B., Chouhan, G., Moiemen, N. S. & Grover, L. M. Advances in keratinocyte delivery in burn wound care. *Adv. Drug Deliv. Rev.* **123**, 18–32 (2018).
32. Sabri, A., Dabbous, H., Dowli, A. & Barazi, R. THE AIRWAY IN INHALATIONAL INJURY: DIAGNOSIS AND MANAGEMENT. *Ann. Burns Fire Disasters* **XXX**, 24–29 (2017).
33. Demling, R. H. Smoke inhalation lung injury: an update. *Eplasty* **8**, e27 (2008).
34. Walker, P. F. *et al.* Diagnosis and management of inhalation injury: An updated review. *Crit. Care* **19**, 1–12 (2015).
35. Cohen, M., Bahoric, A. & Clarke, H. M. Aerosolization of epidermal cells with fibrin glue for the epithelialization of porcine wounds with unfavorable topography. *Plastic and Reconstructive Surgery* **107**, 1208–1215 (2001).
36. Hafez, A. T. *et al.* Aerosol transfer of bladder urothelial and smooth muscle cells onto demucosalized colonic segments: A pilot study. *J. Urol.* **169**, 2316–2320 (2003).
37. Thiebes, A. L. *et al.* Flexible Endoscopic Spray Application of Respiratory Epithelial Cells as Platform Technology to Apply Cells in Tubular Organs. *Tissue Eng. Part C Methods* **22**, 322–331 (2016).
38. Kardia, E., Ch'ng, E. S. & Yahaya, B. H. Aerosol-based airway epithelial cell delivery improves airway regeneration and repair. *J. Tissue Eng. Regen. Med.* **12**, e995–e1007 (2018).
39. Kim, S. Y. *et al.* Atomized Human Amniotic Mesenchymal Stromal Cells for Direct Delivery to the Airway for Treatment of Lung Injury. *J. Aerosol Med. Pulm. Drug Deliv.* **29**, 514–524 (2016).
40. Bieber, M. *et al.* Experimental Investigation of Endoscopic Cell Spray. *At. Sprays* **27**, 847–858 (2017).
41. Thiebes, A. L., Albers, S., Klopsch, C., Jockenhoevel, S. & Cornelissen, C. G. Spraying Respiratory Epithelial Cells to Coat Tissue-Engineered Constructs.

Biores. Open Access **4**, 278–287 (2015).
42. Zhou, H. *et al.* Bioengineering Human Lung Grafts on Porcine Matrix. *Ann. Surg.* **267**, 590–598 (2018).
43. Syedain, Z. H., Naqwi, A. A., Dolovich, M. & Somani, A. In vitro evaluation of a device for intra-pulmonary aerosol generation and delivery. *Aerosol Sci. Technol.* **49**, 747–752 (2015).
44. Lachmann, N. *et al.* Gene correction of human induced pluripotent stem cells repairs the cellular phenotype in pulmonary alveolar proteinosis. *Am. J. Respir. Crit. Care Med.* **189**, 167–182 (2014).
45. Racanelli, A. C. & Ding, B. Sen. Manmade macrophage offers a new therapy for pulmonary alveolar proteinosis. *Am. J. Respir. Crit. Care Med.* **198**, 297–298 (2018).
46. Happle, C. *et al.* Pulmonary transplantation of human induced pluripotent stem cell-derived macrophages ameliorates pulmonary alveolar proteinosis. *Am. J. Respir. Crit. Care Med.* **198**, 350–360 (2018).
47. Zhao, L. *et al.* Engineered Tissue–Stent Biocomposites as Tracheal Replacements. *Tissue Eng. Part A* **22**, 1086–1097 (2016).
48. Jones, M. C. *et al.* Defining the biomechanical properties of the rabbit trachea. *Laryngoscope* **124**, 2352–2358 (2014).
49. Zvarova, B. *et al.* Residual Detergent Detection Method for Nondestructive Cytocompatibility Evaluation of Decellularized Whole Lung Scaffolds. *Tissue Eng. Part C Methods* **22**, 418–428 (2016).
50. Butler, C. R. *et al.* Vacuum-assisted decellularization: an accelerated protocol to generate tissue-engineered human tracheal scaffolds. *Biomaterials* **124**, 95–105 (2017).
51. Hendriks, J. *et al.* Optimizing cell viability in droplet-based cell deposition. *Sci. Rep.* **5**, 1–10 (2015).
52. Bieber, M. *et al.* Viability of coaxial atomization for disintegration of cell solutions in cell spray applications. (2017). doi:10.4995/ilass2017.2017.4609
53. Veazey, W. S., Anusavice, K. U. & Moore, K. Mammalian cell delivery via aerosol deposition. *J. Biomed. Mater. Res. - Part B Appl. Biomater.* **72**, 334–338 (2005).
54. Kardia, E., Yusoff, N. M., Zakaria, Z. & Yahaya, B. Aerosol-Based Delivery of Fibroblast Cells for Treatment of Lung Diseases. *J. Aerosol Med. Pulm. Drug Deliv.* **27**, 30–34 (2013).
55. Conconi, M. T. *et al.* Tracheal matrices, obtained by a detergent-enzymatic method, support in vitro the adhesion of chondrocytes and tracheal epithelial cells. *Transpl. Int.* **18**, 727–734 (2005).
56. Maughan, E. F. *et al.* Autologous Cell Seeding in Tracheal Tissue Engineering. *Curr. Stem Cell Reports* **3**, 279–289 (2017).
57. Rashid, M. ur & Coombs, K. M. Serum-reduced media impacts on cell viability and protein expression in human lung epithelial cells. *J. Cell. Physiol.* **234**, 7718–7724 (2019).
58. Ruoslahti, E. Integrins. *J. Clin. Invest.* **87**, 1–5 (1991).
59. Hynes, R. O. Integrins: Versatility, Modulation, and Signaling in Cell Adhesion. *Cell* **69**, 11–25 (1992).
60. Hamilton, N. J. I. *et al.* Using a Three-Dimensional Collagen Matrix to Deliver Respiratory Progenitor Cells to Decellularized Trachea In Vivo. *Tissue Eng. Part C Methods* **25**, 93–102 (2019).
61. Li, Y., Meng, H., Liu, Y. & Lee, B. P. Fibrin gel as an injectable biodegradable scaffold and cell carrier for tissue engineering. *Sci. World J.* **2015**, (2015).

62. Assmann, A. *et al.* Acceleration of autologous invivo recellularization of decellularized aortic conduits by fibronectin surface coating. *Biomaterials* **34**, 6015–6026 (2013).
63. Aoshiba, K., Rennard, S. I. & Spurzem, J. R. Fibronectin supports bronchial epithelial cell adhesion and survival in the absence of growth factors. *Am. J. Physiol. Cell. Mol. Physiol.* **273**, L684–L693 (1997).
64. Scarritt, M. E., Pashos, N. C. & Bunnell, B. A. A review of cellularization strategies for tissue engineering of whole organs. *Front. Bioeng. Biotechnol.* **3**, 1–17 (2015).
65. Delgado, O. *et al.* Multipotent capacity of immortalized human bronchial epithelial cells. *PLoS One* **6**, 1–8 (2011).